# Two mutations in mitochondrial *ATP6* gene of ATP synthase, related to human cancer, affect ROS, calcium homeostasis and mitochondrial permeability transition in yeast

Katarzyna Niedzwiecka[1], Renata Tisi[2,3], Sara Penna[2§], Malgorzata Lichocka[1], Danuta Plochocka[1], Roza Kucharczyk[1]*

[1]Institute of Biochemistry and Biophysics, Polish Academy of Sciences, Warsaw, Poland

[2]Dept. Biotechnology and Biosciences, University of Milano-Bicocca, Milan, Italy

[3]Milan Center for Neuroscience, Milan, Italy

§ now San Raffaele Telethon Institute for Gene Therapy, Scientific Institute HS San Raffaele, Milan, Italy

*Corresponding author

E-mail: roza@ibb.waw.pl, Phone: +48 22 5921221, Fax: +48 22 6584636

## Abstract

The relevance of mitochondrial DNA (mtDNA) mutations in cancer process is still unknown. Since the mutagenesis of mitochondrial genome in mammals is not possible yet, we have exploited budding yeast *S. cerevisiae* as a model to study the effects of tumor-associated mutations in the mitochondrial *MTATP6* gene, encoding subunit 6 of ATP synthase, on the energy metabolism. We previously reported that four mutations in this gene have a limited impact on the production of cellular energy. In this paper, we report the biochemical analysis of strain bearing a fifth cancer related mutation in this gene and show that two of these mutations, Atp6-P163S and Atp6-K90E (human MTATP6-P136S and MTATP6-K64E, found in prostate and thyroid cancer samples, respectively), increase sensitivity of yeast cells both to compounds inducing oxidative stress and to high concentrations of calcium ions in the medium, when Om45p, the component of porin complex in outer mitochondrial membrane (OM), is fused to GFP. In *OM45-GFP* background, these mutations affect the activation of yeast permeability transition pore (yPTP, also called YMUC, yeast mitochondrial unspecific channel) upon calcium induction. Moreover, we show that calcium addition to isolated mitochondria heavily induced the formation of ATP synthase dimers and oligomers, recently proposed to form the core of PTP, which was slower in the mutants. We show the genetic evidence for involvement of mitochondrial ATP synthase in calcium homeostasis and permeability transition in yeast. This paper is a first to show, although in yeast model organism, that mitochondrial ATP synthase mutations, which accumulate during carcinogenesis process, may be significant for cancer cell escape from apoptosis.

**Keywords**: mitochondria, ATP synthase, *ATP6*, *OM45*, cancer, permeability transition

## 1. Introduction

$F_1F_O$-ATP synthase is a highly conserved energy-converting enzyme located in the inner mitochondrial membrane. ATP synthase produces ATP from ADP and inorganic phosphate ($P_i$) in the process of oxidative phosphorylation (OXPHOS) by rotary catalysis using the energy stored in a transmembrane electrochemical gradient [1, 2]. The ~600-kDa monomer of ATP synthase is composed of a soluble $F_1$ domain and a membrane-bound $F_O$ domain [3]. The $F_1$ catalytic domain is formed by the $(\alpha\beta)_3$ hexamer and the central stalk composed of γ, δ and ε subunits, held stationary relative to the membrane $F_O$ region by the peripheral stalk [4, 5]. The $F_O$ domain includes a ring of hydrophobic *c* subunits (10 in yeast), which rotates during catalysis, *a* subunit, forming the proton channel with the *c*-ring, the membrane part of the peripheral stalk, and several small hydrophobic stator subunits (Fig. 1) [6]. Protons flowing through the membrane part of the $F_O$ subcomplex drive the rotation of the *c*-ring [7, 8]. The central stalk transmits the torque generated by *c*-ring rotation to the catalytic head of the $F_1$ subcomplex, where it induces conformational changes of the α and β subunits that result in phosphate bond formation and the generation of ATP. In mitochondria, ATP synthase forms dimers and oligomers in the inner membrane. In fungi, plants, and metazoans, the dimers are V-shaped and associate into rows along the highly curved ridges of lamellar cristae [9-11].

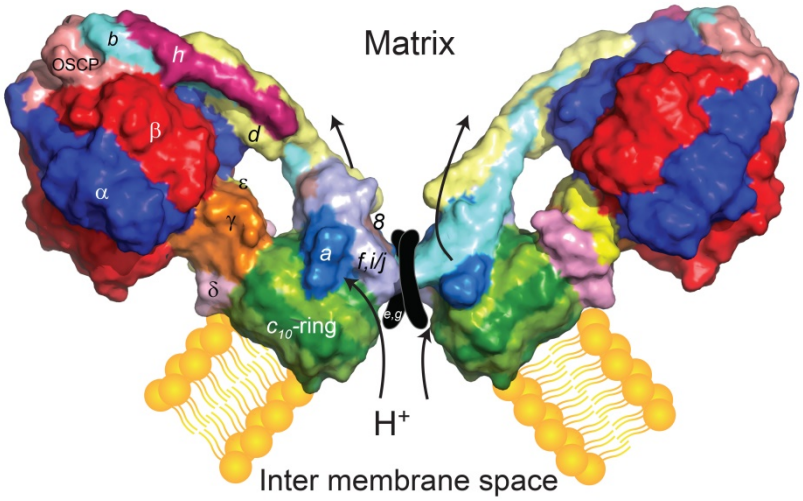


**Figure 1. Schematic diagram of the mitochondrial ATP synthase dimer.** The ATP synthase monomer is organized in three subdomains: the catalytic head $(\alpha\beta)_3$ with the central rotor stalk (γδε); the stator stalk composed of one subunit *b*, subunits *d*, *h*, *f*, *i/j* and OSCP; the Fo membrane domain composed of a ring of subunit *c*/Atp9, subunit *a*/Atp6 and Atp8. The *e* and *g* subunits necessary for the dimerization of ATP synthase are shown. The direction of proton transport during ATP synthesis is indicated.

Defects that result in diminished abundance or functional impairment of the ATP synthase, caused by mutations in nuclear or mitochondrial genes encoding subunits of this enzyme, can cause a variety of severe neuromuscular disorders [12, 13]. Moreover, alterations in mitochondrial genes encoding two subunits of this enzyme, either A6L (Atp8 in yeast) or MTATP6, occur in cancer cells [14, 15]. Although the pathogenic character of mtDNA-encoded complex V mutations leading to myopathies is quite well documented in patient tissues, as well as in cybrid or yeast model cells [16-20], their contribution to cancer development has not been fully explored [21].

The budding yeast *Saccharomyces cerevisiae* is one of the most important model organisms used in fundamental research. It is particularly useful in mitochondrial research, thanks` to its ability to utilize fermentable carbon sources for energy production. This permits yeast cells to survive mutations leading to dysfunction of OXPHOS, allowing their function to be investigated. Moreover, site-directed mutagenesis of its mtDNA is possible, and in contrast to human cells, yeast cells select only one type of mtDNA (homoplasmy), which permits to study the effects of a single mutation. Yeasts have been previously used in our laboratory to study the consequences of pathogenic and cancer-related mutations in mitochondrial ATP synthase *ATP6* gene on OXPHOS functioning [22-29]. Though all the myopathies-related mutations were deleterious for the functionality of yeast ATP synthase, only one cancer-related mutation resulted in a 50% reduction of ATP synthesis at elevated temperature whereas three others had no impact on the energetic function of mitochondria. This result was in accordance with recently published studies showing that OXPHOS activity is preserved and is not the reason of energetic reprogramming in cancer samples, namely their preferences for glycolysis over OXPHOS even in aerobic conditions (the Warburg effect) [30-34].

Since we observed that *ATP6* mutations found in cancer did not interfere with OXPHOS, we hypothesized that they may affect other mitochondrial alterations and/or signaling essential for cancer onset, i.e. calcium/reactive oxygen species (ROS) signaling [35]. Increase of ROS level, albeit not excessive, is beneficial for tumor cells proliferation [36]. ROS production and mitochondrial calcium overload are mutually dependent processes, often disrupted in cancer cells [37, 38]. Although yeast mitochondria do not show high efficiency in calcium uptake, due to the lack of the mitochondrial calcium uniporter (MCU), calcium was actually reported to enter

mitochondria following cytosolic calcium increase [39] suggesting a similar pathway could be active in yeast [40].

The mutual dependency between ROS and calcium is cyclical [41]. This cycle is closed when ROS and calcium trigger permeability transition pore (PTP) opening in mitochondria, that by itself causes a burst of ROS and mitochondrial calcium release together with the apoptosis inducing mitochondrial factors like cytochrome c or endonuclease G [42-44]. PTP is a high-conductance mitochondrial inner membrane channel activated by increased matrix $Ca^{2+}$ levels and oxidative stress, during apoptosis in higher organisms and programmed cell death (PCD) in yeast [45, 46]. The components of the pore are not entirely defined yet, as PTP was induced in targeted gene deletion models of each of the proposed constituents (cyclophilin D, adenine nucleotide translocase-ANT, voltage dependent anion channel-VDAC, Pi-carrier) [47-51]. In recent years, ATP synthase was proposed to form the core of PTP. Two different models were proposed. The first one suggested PTP core be formed by *c*-ring, after a calcium-dependent partial or total dissociation of the $F_1$ from $F_O$ [52, 53], but this hypothesis was recently excluded [54, 55]. The second one assumed that the dimers of ATP synthase can reversibly undergo a calcium-dependent re-modulation to form a channel that mediates the permeability transition [56-59]. Apoptosis is often preceded by activation of autophagy, the process of cytosol or organelles transport to the vacuole for degradation and further recycling. Autophagy is activated by physiological stress, i.e. ROS, and plays a pro-survival role [60]. In the case of mitochondrial dysfunction, loss of autophagy, especially of mitophagy, promotes cancer [61]. Mitophagy can be assessed by using mitochondrial outer membrane protein Om45p tagged with GFP as a marker. In yeast Om45p is in a complex with porin and participates in coordination of transport of many metabolites and ions through both mitochondrial membranes [62, 63].

Here we show that tagging of Om45p is not neutral for the cell and that a genetic interaction occurs between porin complex and Atp6p in yeast. When the functioning of the porin complex is perturbed by the presence of GFP in Om45p, two Atp6 mutations, K90E or P163S (corresponding to lysine 64 or proline 136 in human), increase sensitivity to both oxidative stress and high levels of calcium ions in the medium and slow down the formation of the yeast permeability transition pore homolog (yPTP, YMUC) after calcium induction. This points to a role for ATP synthase, together with

porin complex, in calcium homeostasis and the mitochondrial permeability transition *in vivo*.

## 2. Materials and Methods

### *2.1. Construction of yeast strains and culture conditions*

The strains used in this study are listed in supplementary Table S1. The MR6 strain was used as a wild type control in all experiments. The DFS160 strain bears *kar1-1* mutation that prevents nuclear fusion and enables recombination of mtDNA between the two strains crossed [64]. The $\rho^+$ indicates the wild-type complete mtDNA (when followed by mutation it means the complete mtDNA with a single introduced mutation). The $\rho^-$ synthetic genome was obtained by biolistic introduction into mitochondria of $\rho^o$ DFS160 strain (devoid of mitochondrial DNA) of pTZ18u plasmid (Addgene) encoding wild type *COX2* gene and mutated *atp6-K90E* gene. The construction of RKY61, bearing *atp6-P163S* mutation, was described in Niedzwiecka et al. 2016 [28]. The RKY62 strain, bearing *atp6-K90E* mutation, was obtained exactly by the same strategy as the RKY61, by crossing the RKY59 with the MR10 strain, and the selection of respiring arginine auxotrophic colonies. The sequence of Forward oligonucleotide used for introduction of *atp6-K90E* mutation was: GCTTAAAGGACAAATTGGAGGT**GAA**AATTGAGGTTTATATTTCCCTATG, the Reverse oligonucleotide was complementary to the Forward one. *OM45-GFP* tagging was made as in Kanki et al [65]. Om45p forms a complex with Por1p through Om14p protein [63]. In order to disrupt this complex, we deleted *OM14* gene by integrating the *om14::KANMX4* cassette (encoding an enzyme conferring resistance to geneticin). The cassette was amplified using a total DNA isolated from the *om14::KANMX4* deletion mutant as a template (Euroscarf collection) with the following primers: GTTGCTTATCCGCTTTCTCG and CTTATCACTTGACCGATGAAG. The PCR product was transformed to the wild type, *atp6-P163S* or *atp6-K90E* mutants to delete *OM14*. The verification of correct *OM14* deletion was obtained by PCR with CTGGTATAATTCGTTTCTCAT primer and an internal primer to the *KANMX4* gene. The double mutant *om14::KANMX4 OM45-GFP-KANMX6* was obtained by crossing the single mutants and subsequent sporulation of the diploids and tetrads dissection. To obtain the triple mutants *om14::KANMX4 OM45-GFP atp6-P163S* (KNY41) and *om14::KANMX4 OM45-GFP atp6-K90E* (KNY42), the $\rho^+$ *atp6-P163S* or $\rho^+$ *atp6-K90E*

genomes were transferred by cytoduction from KNY26 or KNY27 *kar1-1* strains, respectively, into the KNY24.

Yeast cells were cultured on fermentative carbon sources: glucose or galactose (to avoid glucose repression of genes encoding respiratory chain proteins). Medium containing galactose is routinely used for growing yeast cells for mitochondria isolation [26]. Glycerol was used as non-fermentable carbon source in respiration media. The media composition was: YPGA (1% Bacto yeast extract, 1% Bacto Peptone, 2% glucose, 40 mg/l adenine), YPGalA (1% Bacto yeast extract, 1% Bacto Peptone, 2% galactose, 40 mg/l adenine), YPGlyA (1% Bacto yeast extract, 1% Bacto Peptone, 2% glycerol, 40 mg/l adenine), W0 complete minimal medium (6.7% Yeast nitrogen base w/o amino acids, 2% glucose, supplemented with complete or drop-out amino acids stock (Sunrise). The liquid media were solidified by addition of 2% of Bacto Agar (Difco, Becton Dickinson). 200 µg/ml of geneticin was added to YPGA plates for selection of *KANMX4 or KANMX6* transformants.

### *2.2. Plasmids used in the study*

Plasmids bearing *PMR1* and *PMC1* genes, encoding the calcium transporters into the Golgi or vacuolar compartment, respectively, were previously described [66]. pVTU-AEQ plasmid, which encodes cytoplasmic aequorin, was previously described [67]. pMTS-AEQ plasmid was constructed from pVTU-AEQ plasmid. Mitochondria targeting sequence (MTS) was amplified in a PCR reaction with Mts-AEQup primer: AGAGCTCATGGCATCTACCAGAGTATTAGCC, bearing SacI restriction site added to the 5` end, and Mts-AEQlow fusion primer: GGCTAGCATAATCAGGAACATCATAAAGCTTGGCCCTCTTTTGCGTAATCTGTC (sequence of apoaequorin cDNA is underlined), using pAM19 plasmid as a template [68]. The PCR product was digested with SacI enzyme and ligated to pVTU-AEQ plasmid digested with KpnI and SacI, present upstream of the sequence encoding aequorin. One-side ligation was performed and the ligation mixture was transformed into yeast MR6 strain by lithium acetate method for homologous recombination of the ends of resulting linear plasmid, in the 5` region of aequorin gene. The resulting plasmid pMTS-AEQ was recovered from yeast and the correct ligation of MTS with aequorin encoding gene was confirmed by restriction analysis and sequencing. pAMS366 plasmid containing *4xCDRE::LacZ* reporter, was kindly provided by M. Cyert

(Stanford University, USA), and previously described [69]. Plasmid pAS1NB:mt-Rosella encoding mitophagy reporter was kindly provided by R.J. Devenish [70].

### *2.3. Bioluminescence aequorin assay*

For cytosolic and mitochondrial calcium concentration variations, yeast strains transformed with pVTU-AEQ or pMTS-AEQ plasmids were grown overnight at 30°C in W0-Ura medium. 6 OD of cells per experiment were harvested (4000 rpm, 10 minutes) from exponentially growing cultures (OD=0.3, nearly 5-6 x $10^6$ cells/ml), and suspended in 1 ml of culture medium to a density of about $10^8$ cells/ml. The cellular suspension was transferred to a microfuge tube and centrifuged at 7000 rpm for 1.5 minutes. For each treatment, 7.2 × $10^7$ cells were suspended in 10 µl of the culture medium, 50 µM coelenterazine (stock solution 1 µg/µl dissolved in 99.5% methanol, conserved in the dark at −20 °C, Molecular Probes) was added and mixed vigorously, and the suspension was incubated for 20 minutes at room temperature in the dark. Cells were collected by centrifugation at 7000 rpm for 1.5 minutes and washed three times with the medium (200 µl/wash); finally they were suspended in 200 µl of fresh medium. The cellular suspension was transferred into a luminometer tube. Light emission was recorded with a Berthold Lumat LB 9501/16 luminometer at intervals of 10 s for at least 1 minute before and for at least 3 minutes after the addition of 6 mM or 10 mM $H_2O_2$, and converted into calcium concentrations according to Brini et al. [71]. $H_2O_2$ was added only when the signal was stable. For each experiment, aequorin expression and activity were tested by treatment of the same amount of cells with 0.5% Triton X-100 in the presence of 10 mM $CaCl_2$, and then monitoring light emission for 24 minutes. Total light emission was calculated and used to normalize light emission according to the amount of expressed aequorin. All experiments were performed at least in three biological replicates. Parameters calculated from patterns of variation in $[Ca^{2+}]_i$ in different cellular strains were compared to those of the wild type strain by pairwise comparison, and significance was assessed by Student's t-test with Šidák-Bonferroni correction, that indicate p=0.01 as the significant threshold.

### *2.4. Calcineurin activity assay*

Yeast cells bearing pAMS366 plasmid were grown at 28°C in liquid W0 or W0Gala medium to OD=2-3. 50 ml (1.5 x $10^9$ cells)-aliquot of the culture was harvested and the pellet was frozen at -20°C. Samples were thawed, suspended in 700 µl of buffer Z (60 mM $Na_2HPO_4$, 40 mM $NaH_2PO_4$, 10 mM KCl, 1 mM $MgSO_4$, pH 7.0) and vortexed with glass beads 3 x 5 minutes with 2 minutes breaks on ice. The extracts were cleared by

centrifugation (5 minutes, 14000 rpm, 4°C). To measure β-galactosidase activity, 100 µl of each extract was added into 1 ml of buffer Z and incubated at 30°C for 5 minutes, then 200 µl of 0.4% ONPG (*o*-nitrophenyl-β-galactopiranoside, Sigma-Aldrich) in 50 mM Tris-HCl pH 8.0 was added and incubated at 30°C for suitable time (5-130 minutes). The reaction was stopped with 500 µl of 1 M $Na_2CO_3$. Amount of newly created *o*-nitrophenol was measured spectrophotometrically at 420 nm and 560 nm. The results were normalized according to the concentration of protein in the extract, which was measured with Lowry procedure. For each condition, at least three independent biological replicates were performed.

### *2.5. Determination of ROS level in cells*

The cytosolic superoxide ($O_2^-$), hydroxyl ($OH^-$) and peroxynitrite ($ONOO^-$) anions accumulation were measured by flow cytometry using dihydroethidium (DHE, Sigma) [72]. Cells were grown in YPGA, YPGalA or YPGlyA to OD=2-3. 3 OD of cells (3.6 x $10^7$) were then converted to spheroplasts with zymolyase 20T (Nacalai Tesque) for 15 minutes at 36°C in PBS pH 7.5/1 M sorbitol buffer. Spheroplasts were washed twice in the same buffer, diluted to a density of $10^7$ cells/ml in buffer supplemented with 10 µM DHE and incubated with shaking for 2 hours at 28°C, followed by overnight incubation in the fridge. The following day, the spheroplasts were washed and suspended to a concentration of $10^6$ cells/ml, sonicated in ultrasound bath (3 x 3 s) and then analyzed by flow cytometry using BD FACS Calibur. The cytosolic $H_2O_2$ was measured by flow cytometry using 2',7'-dichlorodihydrofluorescein diacetate (H2DCFDA, Life Technologies). Cells were grown overnight in YPGA, YPGalA or YPGlyA to stationary phase, suspended in the same medium with H2DCFDA (5 µg/ml) to a density of $10^6$–$10^7$ cells/ml and grown additional 5 hours. Then cells were washed with PBS pH 7.5, suspended to a density of $10^6$ cells/ml, sonicated as above and analyzed by flow cytometry. 10000 cells were counted in the FL1 channel for each sample.

### *2.6. Measurements of mitochondrial Calcium Retention Capacity (CRC) and PTP kinetics*

Mitochondria were prepared by the enzymatic method as described in [73]. Extramitochondrial $Ca^{2+}$ was measured by Calcium Green-5N (Molecular Probes) fluorescence using a $\lambda_{exc}$ of 505 nm and $\lambda_{em}$ of 530 nm in the presence of calcium ionophore ETH129 (5 µM, stock 5 mM in methanol, Sigma-Aldrich) and fatty acid-free BSA (Sigma-Aldrich) under constant stirring at 28°C using a FLX Spectrofluorimeter (SAFAS, Monaco). Mitochondria were diluted in CRC buffer (250 mM sucrose, 10 mM

Tris-MOPS, 10 µM EGTA-Tris, 5 mM $P_i$-Tris, 1 mM NADH, 5 µM ETH129, 1 µM Calcium Green-5N, 0.5 mg/ml BSA, pH 7.4) to the concentration of 500 µg/ml and 20 µM $CaCl_2$ was added every 20 s. Rapid increase of the fluorescence of Calcium Green was interpreted as release of calcium ions from the mitochondrial matrix to the buffer, likely due to permeability transition. The time needed for PTP opening after induction by 100 µM of calcium chloride in the presence of ETH129 calcium ionophore was assessed by measurement of light dispersion at 660 nm under constant stirring at 28°C (PTP assay). Mitochondria (300 µg/ml) were diluted in PTP buffer (0.3 M mannitol, 10 mM HEPES-KOH, 25 µM EGTA, 0.5 mg/ml fatty acid free BSA, 2 mM $KH_2PO_4$, 2 mM NADH, 5 µM ETH129, pH 7.4) and 100 µM $CaCl_2$ was added. PTP induction caused swelling of mitochondria and decrease in absorbance at 660 nm. For microscopic observation on mitochondrial swelling, mitochondria, isolated from cells grown at 36 °C, were diluted (300 µg/ml) in 20 µl PTP buffer pre-warmed at 28°C containing 100 nM MitoTracker green (Thermo Fisher) and put on a cover glass. After 100 µM $CaCl_2$ addition, the mitochondria were evaluated using a Nikon C1 confocal system built on TE2000E and equipped with a 60× Plan-Apochromat oil immersion objective (Nikon Instruments B.V. Europe, Amsterdam, The Netherlands). MitoTracker green were excited with a Sapphire 488 nm laser (Coherent, Santa Clara, CA, USA) and observed using the 515/530 nm emission filter. The images were collected before and after calcium addition during 10 minutes. Following the deconvolution images were processed using the threshold function of ImageJ software and the area of the individual mitochondrion was calculated using “particle analysis” feature, with a lower limit of 0.5 $\mu m^2$ to exclude any non-mitochondrial material.

### *2.7. BN-PAGE assessment of dimerization of ATP synthase complexes under PTP induction*

PTP assay was performed as above. For each experiment, 450 µg of protein from isolated mitochondria was suspended in 1.5 ml of PTP buffer. 100 µM $CaCl_2$ was added. After 0.5, 1, 2.5 or 5 minutes, 1.33 ml of the reaction (400 µg protein) was collected in a new Eppendorf tube, put onto ice and immediately centrifuged (14000 rpm, 4°C, 5 minutes). The pellet was suspended in 100 µl of Extraction Buffer (30 mM HEPES, 150 mM potassium acetate, 12% glycerol, 2 mM 6-aminocaproic acid, 1 mM EGTA, 2% digitonin (Sigma), protease inhibitor cocktail tablets (Roche), pH 7.4) and incubated for 30 minutes on ice. The extract was cleared by centrifugation (14000 rpm, 4°C, 30 minutes), 4.5 µl of loading dye was added (5% Serva Blue G-250, 750 mM 6-

aminocaproic acid) and 160 µg protein was loaded per lane into NativePAGE™ 3-12% Bis-Tris Gel (Invitrogen) for BN-PAGE electrophoresis. After transfer onto PVDF membrane the ATP synthase complexes were detected by Atp2 antibody (gift from M-F. Giraux, CNRS, Bordeaux, France).

### *2.8. Miscellaneous procedures*

Mitophagy was analyzed according to [65, 70]. To induce mitophagy cells pre-grown in rich glucose medium were transferred to YPGlyA (to assess the amount of processed Om45p-GFP) or W0 – uracil with glycerol medium (for mtRosella plasmid selection) for 3-5 days. Total protein extracts were prepared from cells expressing Om45p-GFP by NaOH/TCA method and the amount of Om45p-GFP and free GFP were assessed by Western blotting using anti-GFP antibody (Roche). Cells expressing mtRosella plasmid were examined every day of growth using an Axio Imager M2 microscope (Zeiss) equipped with 38HE and 20HE filter sets for green and red fluorescence, respectively, and were documented using Axio Vision 4.8. Methods for measurement of mitochondrial respiration, ATP synthesis, hydrolysis and membrane potential were previously described [22, 24]. For BN-PAGE analysis of ATP synthase, 400 µg of mitochondrial proteins were thawed and centrifuged (14000 rpm, 4°C, 5 minutes) to obtain the pellet of crude mitochondria. The pellet was then suspended in 100 µl of Extraction Buffer and processed as above. For SDS-PAGE analysis 50 µg of total protein NaOH/TCA precipitates were loaded per lane of 12% SDS-PAGE gel, transferred onto nitrocellulose membrane and analyzed by Western blotting. For steady-state analysis of calcium pumps, 15 µg of membrane proteins were loaded per gel and processed for Western blot according to [74]. Unless otherwise stated in the figure legends, each experiment was repeated at least three times. Intensity of bands was quantified using ImageJ. Data are presented as average ± s.d. or as representative experiment. Student's t-test was used to assess significant differences with the respective control. Multiple sequence alignment of ATP synthase subunits *a* was performed using COBALT [75]. The homology models of human and yeast *ac* complex are based on the atomic models build in the cryo-electron microscopy density map of the bovine ATP synthase (PDB id: 2HLD) as described in Niedzwiecka et al. [28].

## 3. Results

### 3.1. *atp6-P163S* and *atp6-K90E* mutations lead to oxidative stress and ROS production in *OM45-GFP* background

Previously we have shown that four cancer related mutations in *MT-ATP6* gene in positions m.8914C>A, m.8932C>T, m.8953A>G, m.9131T>C, identified in thyroid, prostate, para-thyroid and breast cancer, respectively, have limited impact on OXPHOS when modeled in yeast (amino acid changes in human MTATP6/yAtp6 proteins: P130/157T, P136/163S, I143/170V, L202/232P, see Fig. S1 for a sequence alignment that shows the 2D positions of the mutations) [28]. One mutation, Atp6-P163S, reduced ATP synthesis rate to 50% of the wild type enzyme in mitochondria isolated from cells grown at elevated temperature. The fifth mutation, changing the conserved lysine 90 into glutamic acid, corresponding to K64 in human MTATP6 protein, identified in thyroid cancer, was found to be neutral for OXPHOS activity as well (supplementary results, Fig. S2) [76]. These mutations were identified in cancer samples, often in homoplasmic state, suggesting that they may be significant for other processes important during tumorigenesis. Since microautophagic vacuolar membrane invaginations and presence of mitochondria in autophagosomes were previously observed in some other *atp6* mutants constructed in our laboratory (*atp6-W136R* and *atp6-L247R*, corresponding to human m.8851T>C and m.9176T>G mutations, leading to FBSN or MILS syndromes, respectively, [24, 26] and unpublished), we also investigated the mitophagy process, often defective or modified in cancers [77]. As a marker of mitophagy we used the Om45p protein fused to GFP in wild type and cancer-related *atp6* mutants strains. Though, we did not observe significant difference in mitophagy rate by this method (supplementary results and Fig. S3).

Identification of hypersensitivity or resistance to inhibitors of growth of yeast mutants can be useful in elucidating the effect of mutations and thus the function of genes within the cell [78]. We screened the *atp6* mutants for growth phenotypes on plates supplemented with different compounds, especially those known for inducing oxidative stress: $H_2O_2$, cumene hydroperoxide, tert-butyl hydroperoxide, rapamycin [79]. Screening also for synthetic lethality, we included the mutants in *OM45-GFP* background, because Om45p is in complex with yeast VDAC homolog, Por1p, expression of which is sometimes up-regulated in cancers [62, 80, 81]. As shown in Fig. 2A, *atp6-P163S OM45-GFP* double mutant grew more poorly on fermentative

media at elevated temperature (36°C), indicating its defective adaptation to heat. Moreover, in the *OM45-GFP* background, two *atp6* mutations, *atp6-K90E* and *atp6-P163S*, increased sensitivity of yeast to hydrogen peroxide and rapamycin, at normal (28°C) and elevated (36°C) temperatures. Rapamycin, by inhibition of the Tor protein kinase, elicits many of the cellular responses that are triggered by nutrient starvation, such as inhibition of protein synthesis, down-regulation of amino acid permeases, protein degradation, autophagy, cell cycle arrest and higher ROS level [82, 83]. These phenotypes suggested ROS detoxification be defective in the double mutants *atp6-K90E OM45-GFP* and *atp6-P163S OM45-GFP*. We thus evaluated the cellular levels of ROS in single and double mutants grown in rich glucose, galactose (fermentation) or ethanol (respiratory) media at both temperatures, using DHE and H2DCFDA probes specific for superoxide anion and hydrogen peroxide, respectively [84, 85]. As positive controls, we used *sod1*Δ strain, deprived of a cytosolic copper-zinc superoxide dismutase that enables cells to detoxify superoxide, for DHE staining [86]; for H2DCFDA staining, the wild type strain treated with antimycin A (in glucose repression conditions) or high concentration of $H_2O_2$ in glucose de-repression conditions were used [87, 88]. Antimycin A treatment induces production of superoxide anion, which is immediately metabolized by Sod1p and Sod2p superoxide dismutases to $H_2O_2$. Neutralization of $H_2O_2$ by catalase T is much slower in glucose than in galactose or ethanol, conditions when catalase A is active (our unpublished observations and [89, 90]). Similar results were obtained for strains grown at 28 and 36°C. Higher ROS level was observed in the double, but not single mutants, grown in rich glucose medium (Fig. 2B), as well as in the control strains. The percentage of ROS accumulating cells in the mutants varied from 40 to 50% of cells in population. When cells were grown in glucose de-repression conditions, i.e. galactose (fermentative) or glycerol (respiratory) media, the percentage of ROS accumulating cells in double mutants reached up to 70%. It is worth mentioning that the single *OM45-GFP* mutant also presented higher ROS level when grown in galactose or respiratory media (from 45 to 60%).

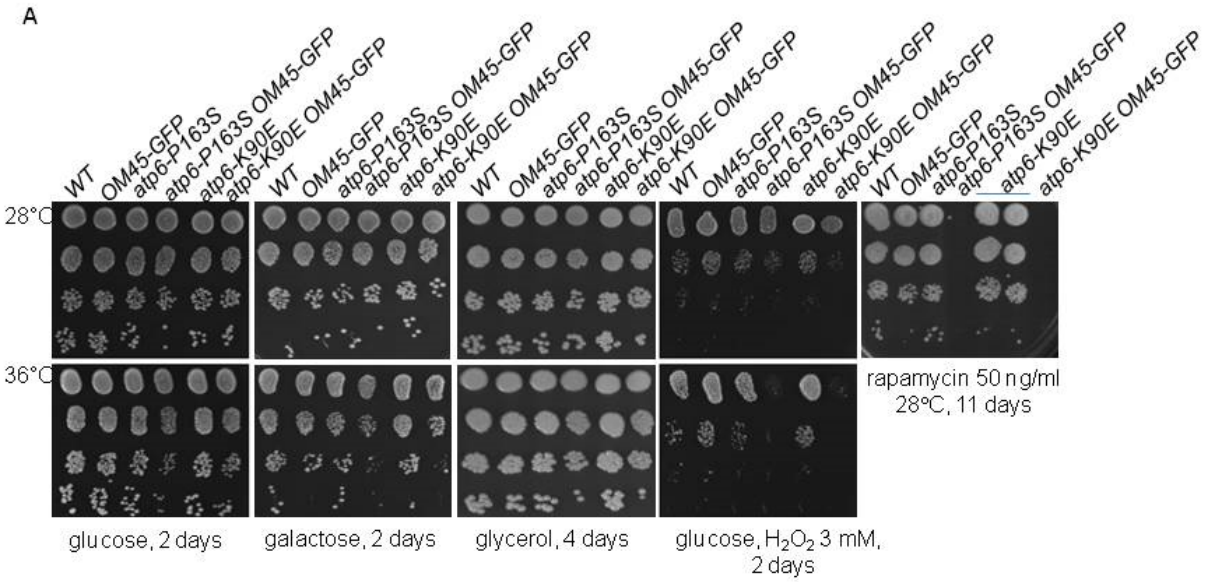


412

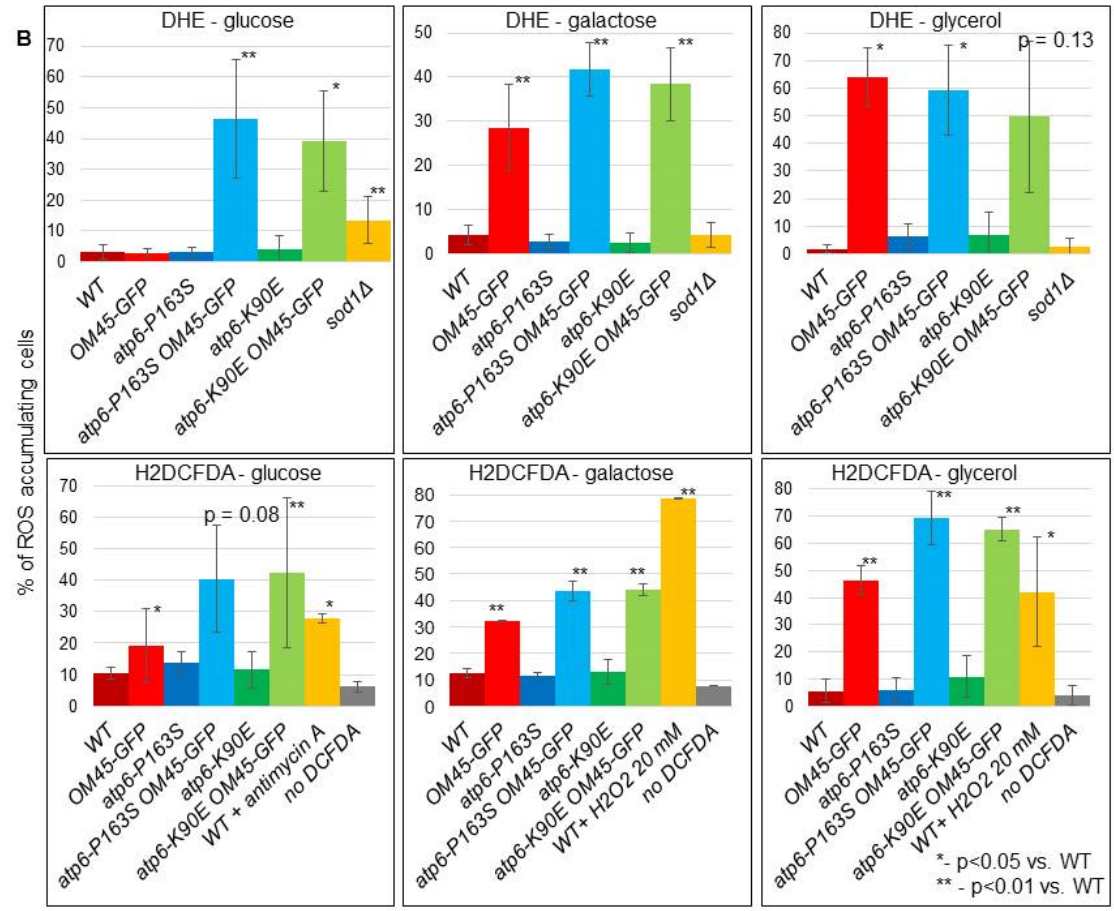


413

414 **Fig. 2. Atp6-K90E and Atp6-P163S mutations in Atp6p lead to increased ROS**
415 **level in Om45-GFP cells.** (**A**) Fresh liquid glucose cultures were serially diluted,
416 spotted onto rich medium plates, incubated at the indicated temperatures and
417 photographed after the indicated number of days. Growth test in the presence of
418 rapamycin is shown only at 28ºC, as it stops growth of *WT* at 36ºC. (**B**) Percentage of

ROS accumulating cells cultured in rich glucose, galactose or glycerol media at 28°C and stained with DHE (upper panel) or H2DCFDA (lower panel), as described in Materials and Methods. As a control, yeast cells deleted for *SOD1* gene were used for DHE staining, and wild type cells treated with 20 µM antimycin A or 20 mM $H_2O_2$ for 45 minutes for H2DCFDA staining. The error bars and p-values versus wild type control were calculated from at least three independent experiments and are indicated.

### 3.2. The ATPase activity of ATP synthase is reduced in double *atp6-P163S OM45-GFP* and *atp6-K90E OM45-GFP* mutants

The higher ROS level in the double *atp6-P163S OM45-GFP* and *atp6-K90E OM45-GFP* mutants may be caused by dysfunction of OXPHOS, although the growth on respiratory medium has not been abolished (Fig. 2A). This does not actually imply that the OXPHOS functions normally, as the activity of ATP synthase needs to be decreased by at least 80% to affect yeast respiratory growth [23, 91]. Thus, the respiratory activities and assembly/stability of ATP synthase were measured in mitochondria from mutant cells grown at 36°C, as only at this temperature the single *atp6-P163S* mutant mitochondria presented decreased respiration and ATP synthesis of about 50% (measured at state 3 with NADH as a respiratory substrate) (Fig. 3A, [28]). In contrast, mitochondria isolated from *atp6-K90E* mutant respired and produced ATP with even higher efficiency comparing to the control mitochondria (Fig. S2B). Surprisingly, the modification of Om45p protein by GFP tag also lead to a reduction of respiration and the rate of ATP synthesis to 40-60% of the control mitochondria. These activities in the double mutants were the same as in single Om45p-GFP mitochondria. In all mutants, the CCCP-induced stimulation of respiration, relative to state 4 (NADH alone), was similar to wild type mitochondria, indicating the lack of passive permeability for protons of the inner mitochondrial membrane (Fig. 3A, upper panel). The maximal rate of mitochondrial ATP hydrolysis was then measured, in non-osmotically protected mitochondria buffered at pH 8.4 and in the presence of saturating amounts of ATP. In fact, a pH value of 8.4 is optimal for the $F_1$-ATPase activity and prevents binding of $F_1$ inhibitor protein Inh1 ($IF_1$) to ATP synthase [92]. Furthermore, in these conditions the $F_1$-ATPase is not constrained by any proton gradient across the inner mitochondrial membrane. In control and single mutants mitochondria, the maximal ATPase activity was at the same level and dropped to about 50% in the presence of oligomycin. The maximal ATPase activity was considerably reduced in *atp6-P163S OM45-GFP* and

*atp6-K90E OM45-GFP* double mutants, to 70% of the control mitochondria, but was more efficiently inhibited by oligomycin than in control or single mutants mitochondria (60% vs 40-50%), indicating that ATP synthase complexes are more stable in these mutants (Fig. 3A). According to this, a lower ratio between free $F_1$ and fully assembled enzyme is present in *atp6-P163S OM45-GFP* and *atp6-K90E OM45-GFP* mutants than in control mitochondria (Fig. 3B). The amount of fully assembled enzyme in *atp6-P163S* mutant, assessed by the steady state analysis of Atp6p, which is immediately degraded when not incorporated into the complex, is not further decreased by *OM45-GFP* mutation [93]. The amount of ATP synthase subunits and ATPase inhibitor protein Inh1 bound to $F_1$ was unchanged (Fig. 3B,C).

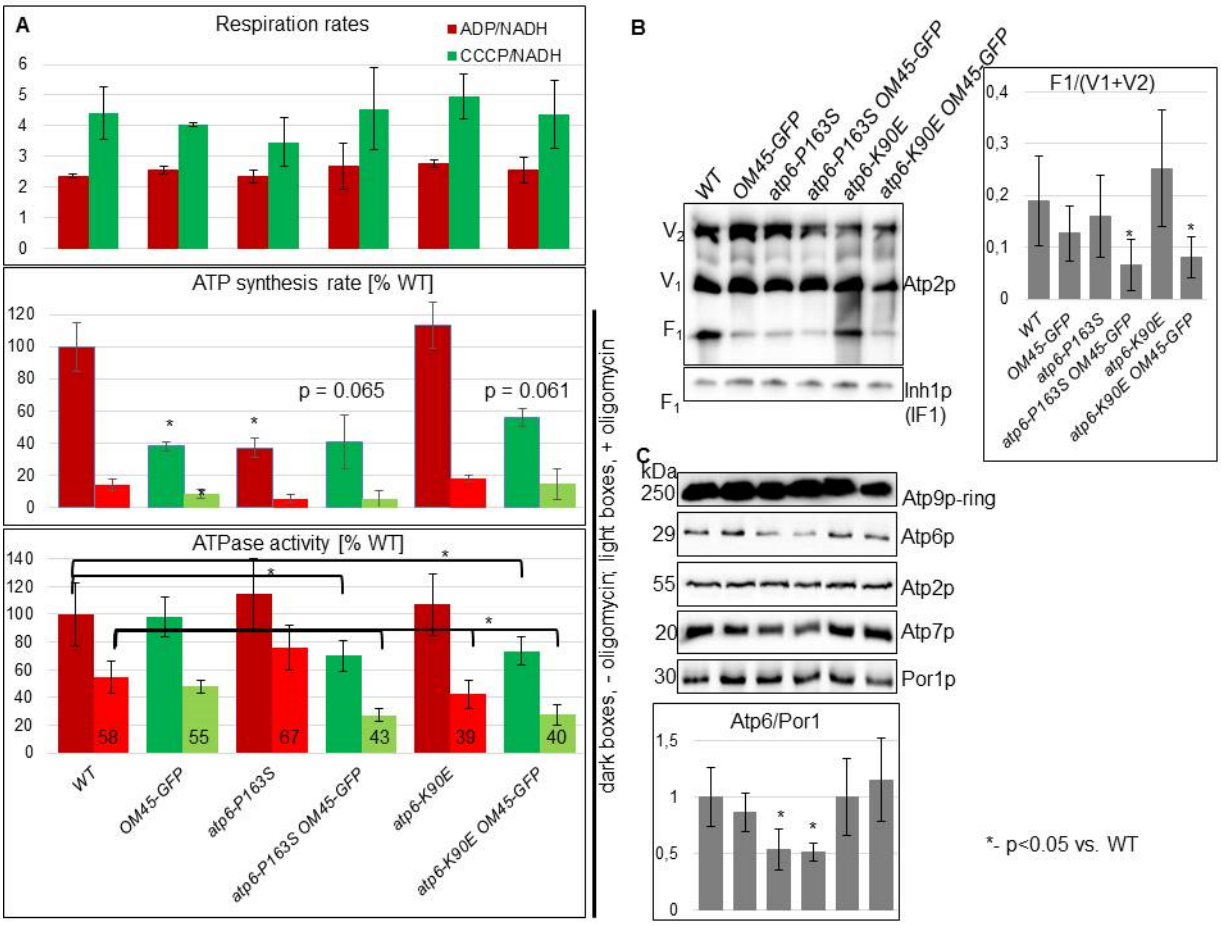


**Fig. 3. ATPase activity is reduced in the double *atp6-P163S OM45-GFP* and *atp6-K90E OM45-GFP* mutants.** (**A**) Mitochondria were isolated from strains grown in rich galactose medium, at 36°C. Oxygen consumption rates were measured after consecutively adding 4 mM NADH (state 4 respiration), 150 µM ADP (state 3) or 4 µM carbonyl cyanide m-chlorophenylhydrazone (CCCP) (uncoupled respiration). The rates of ATP synthesis were determined using 4 mM NADH and 750 µM ADP, in the

presence/absence of 3 mM oligomycin. For the ATPase assays, mitochondria kept at –80°C were thawed and the reaction was performed in the absence of osmotic protection at pH 8.4. The respiratory activities are presented as a ADP/NADH and CCCP/NADH ratio, ATP synthesis and hydrolysis activities (darker rectangles) are expressed in percentage with respect to wild type mitochondria, whereas the activities in the presence of oligomycin (lighter rectangles) are expressed as the percentage of corresponding activities without the drug and are indicated. (**B,C**) BN- and SDS-PAGE analysis of ATP synthase complexes, subunits and Inh1 ATPase inhibitor bound to $F_1$. Dimeric ($V_2$), monomeric ($V_1$) $F_1F_O$ complexes, free $F_1$ and separate subunits were revealed by Western blot with indicated antibodies. The error bars represent standard errors calculated from four independent experiments, the p values were calculated versus wild type control, or the single mutants where indicated. P value for the percentage of ATPase activity inhibition by oligomycin was calculated separately and is indicated. The representative gels are shown.

### 3.3. *atp6-P163S* and *atp6-K90E* mutations affect calcium homeostasis in *OM45-GFP* background

ROS and calcium homeostasis were suggested to interplay in the cellular signaling and development of diseases [94-97]. Thus, calcium sensitivity was verified for single and double mutants. The *atp6-P163S OM45-GFP* and *atp6-K90E OM45-GFP* double mutants were not able to grow on medium supplemented with high concentrations of calcium ions, particularly at the restrictive temperature of 36°C, while the single mutants were growing as well as the control strain (Fig. 4A). This phenotype was suppressed by the overexpression of calcium pumps such as Pmc1p and, albeit less efficiently Pmr1p, which decrease the level of cytosolic calcium concentration by pumping calcium into the vacuole or Golgi compartments, respectively (Fig. 4B). The calcium sensitivity of the mutants was ROS-dependent as addition of ROS scavengers suppressed calcium sensitivity (Fig. 4A).

We wondered if the observed phenotype could be linked to the function of the whole porin complex, which may be impaired by the modification of the C-terminal part of Om45p by GFP. To answer this question we deleted *OM14* gene in double mutants, thus disrupting the bridge connecting Om45p-GFP to Por1p. As shown in Fig. 4C, rapamycin and calcium sensitivities of the double *atp6-P163S OM45-GFP* and *atp6-K90E OM45-GFP* mutants were suppressed by the lack of Om14p. Thus, the presence

of GFP tag at the C-terminal part of Om45p provokes an unknown defect in the whole Por1p-Om14p-Om45p protein complex functioning which is responsible for the observed phenotypes in *atp6-K90E OM45-GFP* and *atp6-P163S OM45-GFP* double mutants.

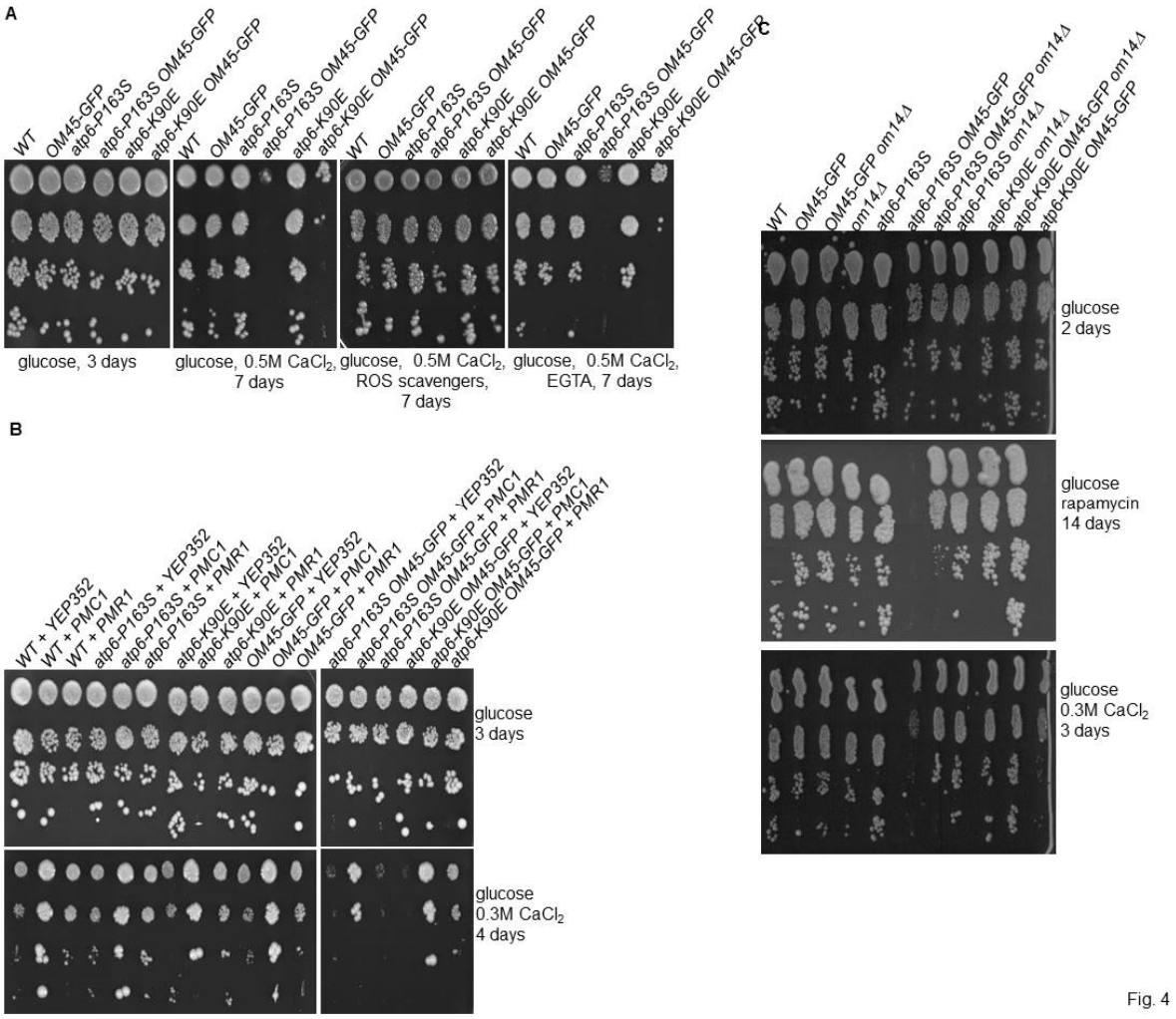


Fig. 4

**Fig. 4. Atp6-K90E and Atp6-P163S mutations in Atp6p lead to increased sensitivity to calcium ions when porin complex is modified by Om45p-GFP.** Precultures in glucose rich (**A,C**) or minimal medium without uracil for plasmid selection (**B**), were serially diluted and spotted onto rich medium with glucose, or glucose supplemented with either 0.3M or 0.5M $CaCl_2$, rapamycin 50 ng/ml, or 0.5M $CaCl_2$ together with either ROS scavengers (5 mM L-ascorbic acid, 5 mM L-cystein, 5 mM reduced L-glutathione and 5 mM N-acetyl-L-cysteine) or 10 mM EGTA, as indicated. Plates were photographed after the indicated number of days of incubation at 36°C, except for rapamycin plate, which was incubated at 28°C. The difference in growth of

518 the double *atp6-P163S OM45-GFP* or *atp6-K90E OM45-GFP* mutants on medium
519 supplemented with 0.3M $CaCl_2$ on (**B**) and (**C**) is due to different medium: minimal (**B**)
520 or complete (**C**).

521 Then, we measured the concentration of calcium in cytosol and mitochondrial
522 matrix in yeast cells *in vivo*, by using aequorin, a luminescent protein. Consistently with
523 previously reported results [39], and in sharp contrast to mammalian cells, cytosolic
524 and mitochondrial resting calcium concentrations in yeast living cells are quite similar,
525 despite a very steep electrochemical gradient toward calcium entry into the
526 mitochondrial compartment. In this condition, only *atp6-P163S OM45-GFP* mutant
527 showed significantly higher calcium concentration both in cytosol (130% vs. wild type)
528 and in mitochondrial matrix (two-fold) (Fig. 5A,B). As calcium sensitivity of the mutants
529 was ROS-dependent (Fig. 4A), we monitored calcium flux upon oxidative stress
530 induced by addition of 10 mM $H_2O_2$. A rapid increase of $Ca^{2+}$ concentration in both
531 cytosol and mitochondrial matrix was observed, then it slowly decreased, and finally
532 achieved a new plateau level which was higher than the basal level. In comparison to
533 the wild type strain, the new plateau level was two-times higher for cytosolic calcium
534 concentration in *atp6-P163S OM45-GFP* mutant and for the mitochondrial matrix
535 calcium concentration in both *atp6-P163S OM45-GFP* and *atp6-K90E OM45-GFP*
536 mutants. This experiment further confirmed the defect in calcium homeostasis
537 regulation in the double mutants.

538 In response to stress, cytosolic calcium concentration increases and calcium
539 ions bind calmodulin, which activates calcineurin [98, 99]. Consequently, calcineurin
540 dephosphorylates the Calcineurin Response Zinc finger transcription factor (Crz1p),
541 which activates expression of several stress response genes controlled by promoters
542 containing Calcineurin-Dependent Response Element (CDRE) sequences. Thus, the
543 $Ca^{2+}$/calmodulin/calcineurin pathway activity was assessed using *lacZ* reporter gene
544 under the control of an artificial *4xCDRE* containing promoter expressed from plasmid.
545 Surprisingly, in glucose medium, calcineurin activity was-three times lower in the *atp6-*
546 *P163S OM45-GFP* strain in comparison to wild type strain, despite the inability of this
547 mutant to maintain a proper resting cytosolic calcium concentration (Fig. 5C). In the
548 absence of glucose repression (on galactose), when Crz1p is free from PKA-
549 dependent inhibition [100], calcineurin-dependent Crz1p activity was three-times lower
550 in the *atp6-P163S OM45-GFP* mutant, but also two-times lower in the *atp6-K90E*

*OM45-GFP* mutant in comparison to wild type strain. This suggests that the higher calcium cytosolic and mitochondrial concentrations may be caused by a defect in calcineurin activation. Expression of calcineurin-dependent calcium transporters could also be affected by calcineurin activity reduction. We assessed the Pmr1p, Pmc1p, Yvc1p, and Vcx1p levels in total membrane extracts from glucose grown cells by Western blotting. The level of these calcium transporters was not reduced in double mutants (Fig. 5D) [74]. Taken together, these data demonstrate that both *atp6-P163S* and *atp6-K90E* mutations impair calcium homeostasis in *OM45-GFP* cells. This effect is indeed less severe for the *atp6-K90E OM45-GFP* mutant, and while it is not evident during exponential growth on glucose, it is observed under glucose derepression (Fig. 5C) or oxidative stress conditions (Fig. 5B).

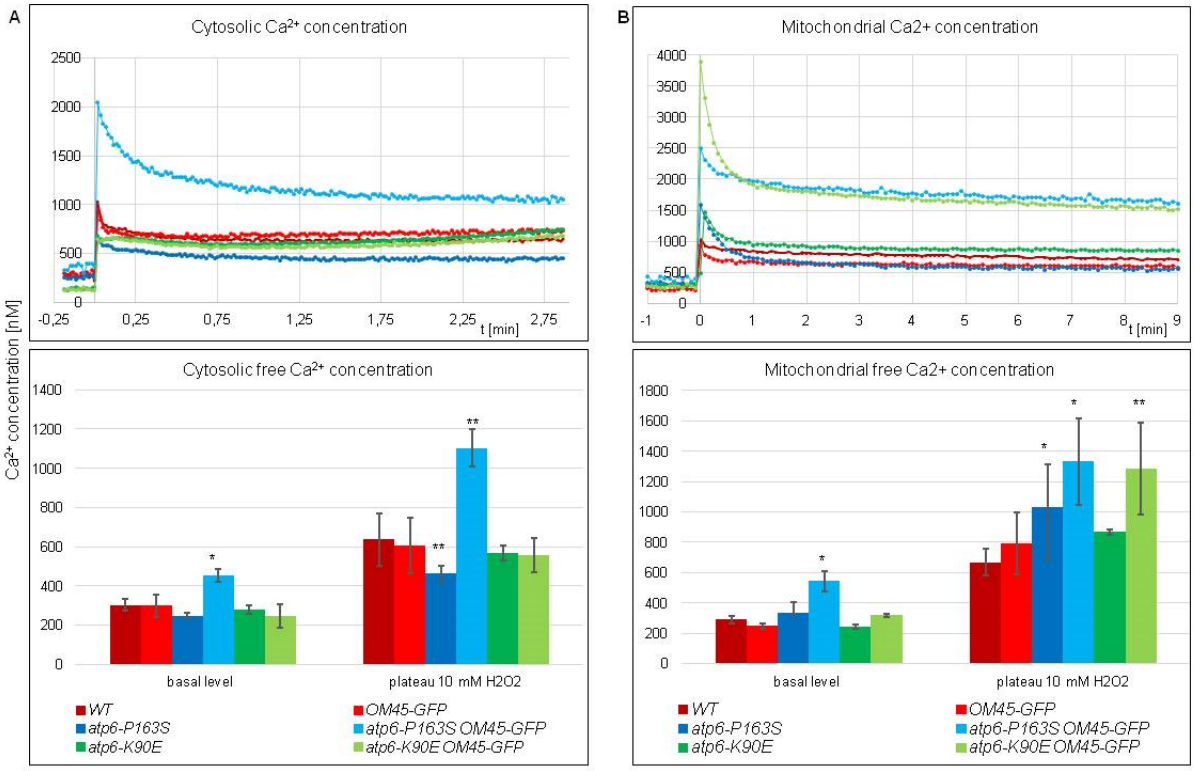

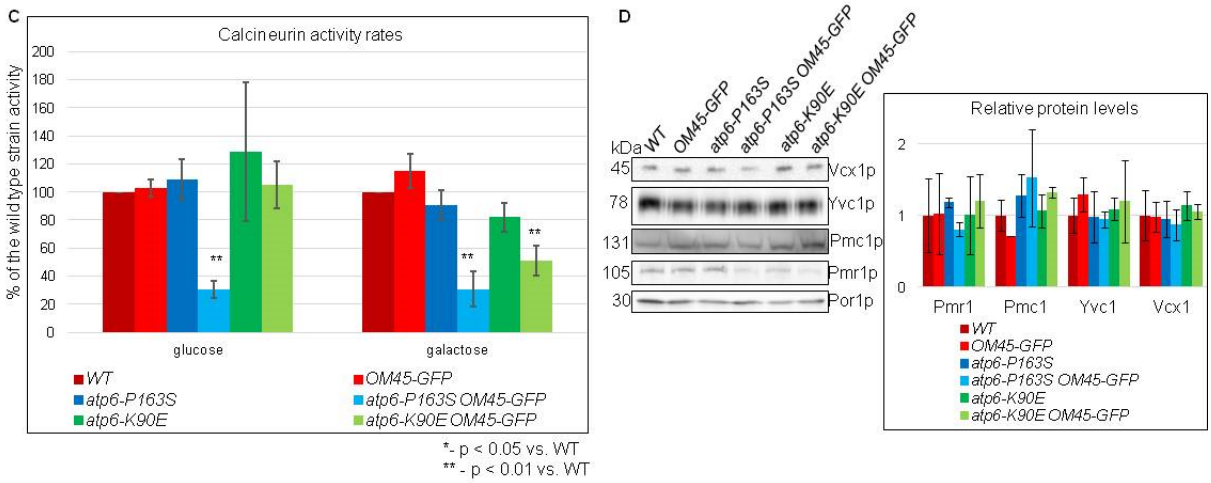


**Fig. 5. Cytosolic and mitochondrial calcium concentration is elevated in double mutants *atp6-P163S OM45-GFP* and *atp6-K90E OM45-GFP*.** Yeast cells with plasmids encoding cytoplasmic aequorin (**A**), mitochondrial aequorin (**B**) or *4xCDRE::lacZ* reporter (**C**) were grown on minimal glucose or galactose medium without uracil at 28°C to early logarithmic phase (**A, B**) or to late logarithmic phase (**C**). (**A, B**) Apoaequorin-expressing cells were loaded with coelenterazine (see Materials and Methods) and the luminescence of aequorin was measured before and after addition of 10 mM $H_2O_2$. (**C**) Protein extracts were prepared using glass beads and proceeded to calcineurin activity assay. (**D**) Proteins (15 µg) from the membrane-enriched fractions of exponentially glucose grown cells ($OD_{600}$ = 1.2) of the indicated strains were separated by SDS-PAGE and transferred to nitrocellulose membrane, which were then immunoblotted with antibodies against Pmc1p, Pmr1p, Vcx1p, Yvc1p and Por1 as a loading control. The error bars and p-values in comparison to wild type indicated by * were calculated from at least three independent experiments.

### 3.4. *atp6-P163S* and *atp6-K90E* mutations influence yPTP induction by calcium in *OM45-GFP* background

The process in which ROS, calcium and ATP synthase are all engaged is the permeability transition [56, 57, 101, 102]. The induction and regulation of the PTP are evolutionary conserved and ATP synthase dimers were found to form yPTP *in vitro*, while the deletion of subunits *e* or *g,* necessary for dimer formation, affected its induction [103]. We thus investigated the PTP induction in the *atp6-P163S* and *atp6-K90E* mutants in *OM45-GFP* background by two assays. The *tim11Δ* strain, lacking

the non-essential *e* subunit of ATPase, in which PTP induction delay is documented, was included as a positive control, but to the experiment performed at 28°C only, because of high instability of mtDNA in this strain at elevated temperature (75% of $\rho^o$ cells versus 55% at 28 °C) [103]. In each assay, the ETH129 ionophore was added, since this is required to allow $Ca^{2+}$ uptake by energized yeast mitochondria [104]. The mitochondria were isolated from all strains the same day, as the variability in growth conditions and mitochondria preparation process influenced the results of the assays very strongly. We performed the analysis at two temperatures, as calcium and $H_2O_2$ sensitivities were more pronounced at elevated temperature (Fig. 2, 4). At first, the propensity of the yPTP to open was assessed based on the calcium retention capacity (CRC), i.e. the maximal $Ca^{2+}$ load retained by mitochondria before onset of the permeability transition [105]. The energized yeast mitochondria were allowed to accumulate $Ca^{2+}$, provided as a train of pulses of 20 µM concentration, until onset of the permeability transition, which causes depolarization followed by rapid $Ca^{2+}$ release from mitochondria and increase of its concentration in the buffer. As shown in Fig. 6A and S4, the CRC was slightly lower (of 20 µM of calcium) in the mitochondria of single *atp6-K90E* and slightly higher (of 20 µM of calcium) in the mitochondria of double *atp6-P163S OM45-GFP* mutants grown at both temperatures, the difference not being statistically significant. The CRC results for other strains mitochondria were not different from wild type mitochondria. Next, we measured the time of PTP opening after calcium stimulation by the mitochondrial swelling assay. The CRC experiment indicated that 100 µM concentration of calcium chloride is enough to open yPTP. Thus the swelling assay was performed with this concentration of calcium ions to measure the time required for induction of the permeability transition. After addition, calcium lead to the rapid increase in the dispersion of the 660 nm wave [106]. Then, after a few minutes, PTP opens (indicated by arrows on Fig. S4) allowing the equilibration of sucrose and water across mitochondrial membrane and the swelling of mitochondria manifesting in a fast decrease in absorbance. In accordance to CRC assay, calcium induced the permeability transition in mitochondria of single *atp6-K90E* mutant in a shorter time than in wild type mitochondria (after about 60% of the time needed by wild type mitochondria, at elevated temperature). Surprisingly, the permeability induction in mitochondria of both *atp6-K90E OM45-GFP* and *atp6-P163S OM45-GFP* mutants was delayed in comparison to wild type mitochondria, when isolated from cells grown at elevated temperature. The mutant mitochondria needed two-fold longer time to open

the channel (Fig. 6B). This effect, although less pronounced, was also seen in mitochondria isolated from *atp6–P163S OM45-GFP* mutant cells grown at 28ºC.

To further confirm this result we have observed swelling of mitochondria from wild type, *atp6–P163S OM45-GFP* and *atp6-K90E (stained* with MitoTracker green) under confocal microscopy. Before calcium addition the size of mitochondria varied between 0.5 -1.5 $\mu m^2$, with no significant difference among the strains. Immediately after calcium addition, mitochondria started swelling and their diameter visibly increased, and finally ruptured, causing their number to decrease. Thus, the amount of swollen mitochondria was quantified after one minute after calcium addition. As shown in Fig. 5C, 40% of wild type mitochondria were swollen at this time-point, comparing to 30% of double mutant *atp6-P163S OM45-GFP* and 60% of single mutant *atp6-K90E* mitochondria. This experiment further confirmed the impact of *atp6* mutations and *OM45-GFP* tagging on permeability transition in yeast mitochondria.

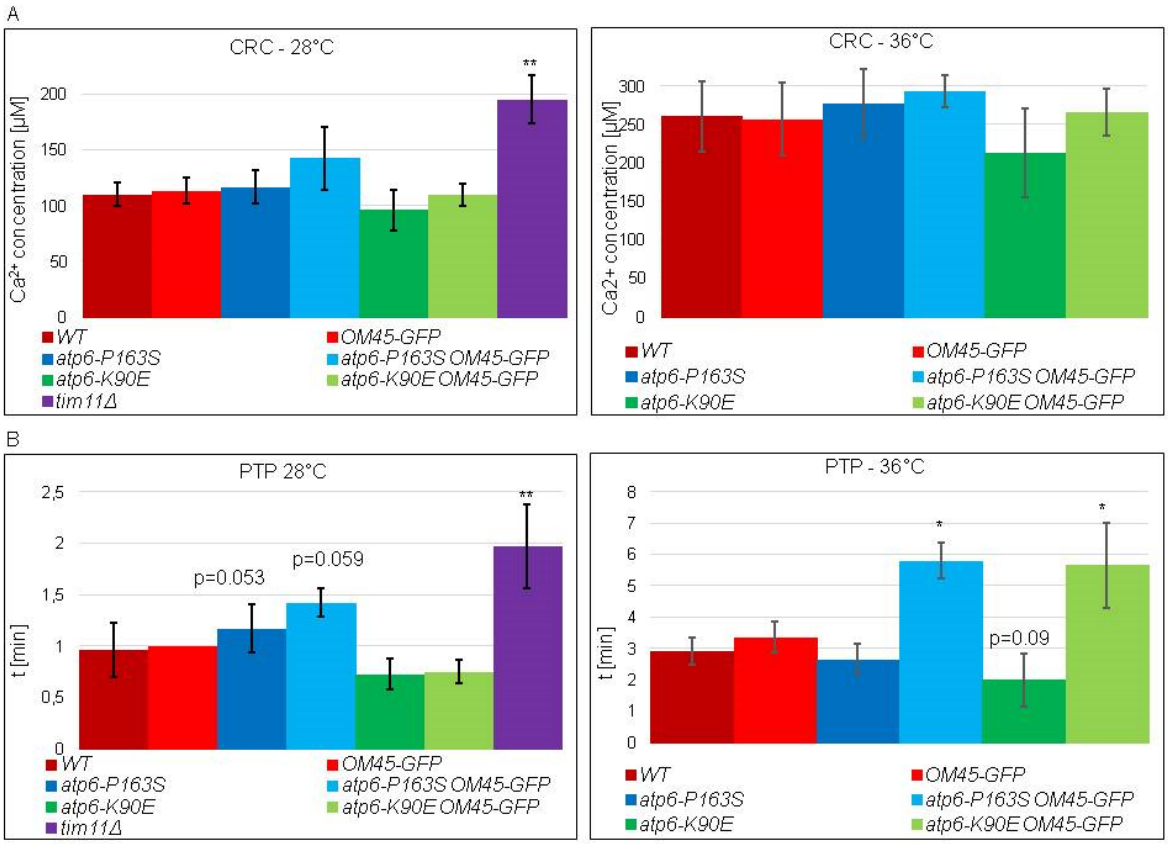


* - p < 0.05; ** - p < 0.01 vs. WT

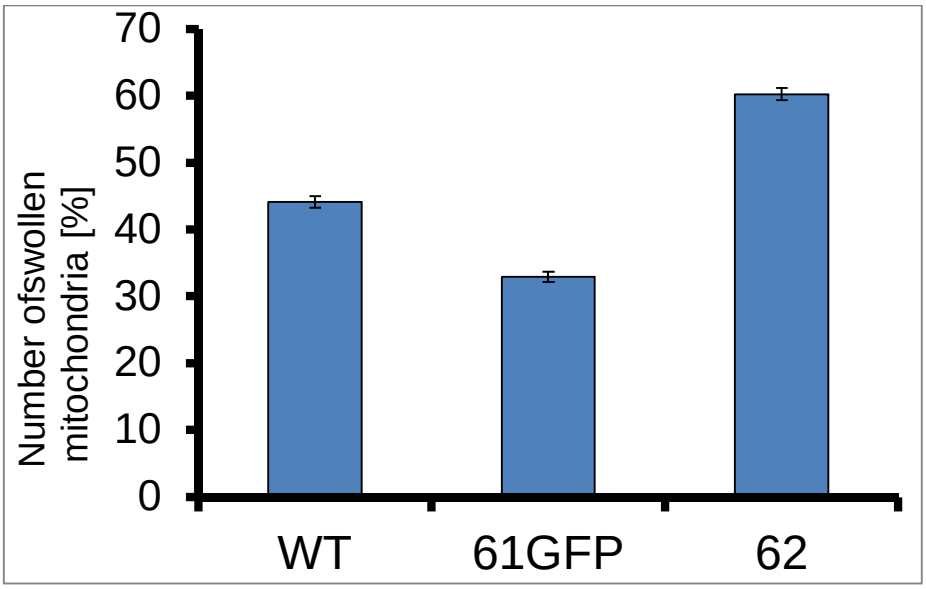


**Fig. 6. Properties of the permeability transition in yeast mitochondria.** (**A**) Calcium retention capacity of yeast mitochondria calculated basing on CRC assay. The differences between strains are not statistically significant. (**B**) Time of PTP opening after calcium stimulation basing on swelling assay. Data are average of at least four independent experiments. The corresponding traces are shown in supplementary results Fig. S4. (**C**) Swelling of mitochondria observed under confocal microscopy and shown as percentage of enlarged mitochondria (> 1.5 $\mu m^2$) at 1 minute time-point after addition of $CaCl_2$. Data are average of three independent experiments. The asterisks indicate the statistical significance of the difference between mutants and the wild type.

### 3.5. *atp6-P163S* and *atp6-K90E* mutations modulate the dynamics of ATP synthase dimers/oligomers formation during yPTP induction in *OM45-GFP* background

The observed differences in time of PTP opening after calcium induction might be due to different dynamics of ATP synthase dimers/oligomers formation. We repeated the swelling assay at elevated temperature and the reaction was stopped at different times-points by putting mitochondria on ice and immediately extracting ATP synthase complexes for BN-PAGE analysis (Fig. 6B). Only strains with different PTP opening time compared to control mitochondria were picked for analysis - *atp6-K90E* and *atp6-P163S OM45-GFP*, in order to guarantee fast processing of samples during the same experiment. The strong induction of the oligomerization of ATP synthase is already evident 30 s after calcium addition in wild type mitochondria. As expected, in the *atp6-K90E* single mutant mitochondria the induction of dimerization/oligomerization

659 of ATP synthase by calcium ions was faster than in control mitochondria, whereas in
660 the double *atp6-P163S OM45-GFP* mutant mitochondria it was slower (Fig. 7).
661 Furthermore, a different ratio of dimers and oligomers to monomers was observed in
662 mutants. In single *atp6-K90E* mutant, more dimeric and mainly oligomeric forms were
663 present after 30s until 2.5 minutes from the start of the reaction. In particular there is
664 more oligomers in that mutant. At the 5 minutes time point, the same ratio for the
665 mutant and wild type control was reached. This is consistent with the faster PTP
666 induction observed in this mutant (Fig. 6B, S4B right panel, green line). Conversely, in
667 the double mutant *atp6-P163S OM45-GFP* the appearance of dimers/oligomers was
668 slower in comparison to wild type mitochondria (Fig. 7); again, this correlates with the
669 permeabilization of mitochondrial outer membrane, which only started after 5 minutes
670 in this mutant (Fig. 6B, S4B right panel, light blue line). The ratio of dimers/oligomers
671 to monomers was growing till 1 minute-time point in wild type mitochondria while until
672 2.5 minutes-time point in the mutant mitochondria. After reaching the maximum value
673 this ratio dropped and at the time-point of PTP opening was similar for all strains
674 mitochondria. This experiment has clearly showed that i) calcium induction of
675 permeability transition in yeast native mitochondria correlates with changes in the
676 oligomerization states of ATP synthase, ii) *atp6-K90E* and *atp6-P163S* mutations of
677 ATP synthase subunit *a*/Atp6 impinges on the dynamic of this changes iii) Om45p, a
678 component of the yeast VDAC homolog Por1p complex (Por1p-Om14p-Om45p), has
679 a significant role in this process.

Fig. 7

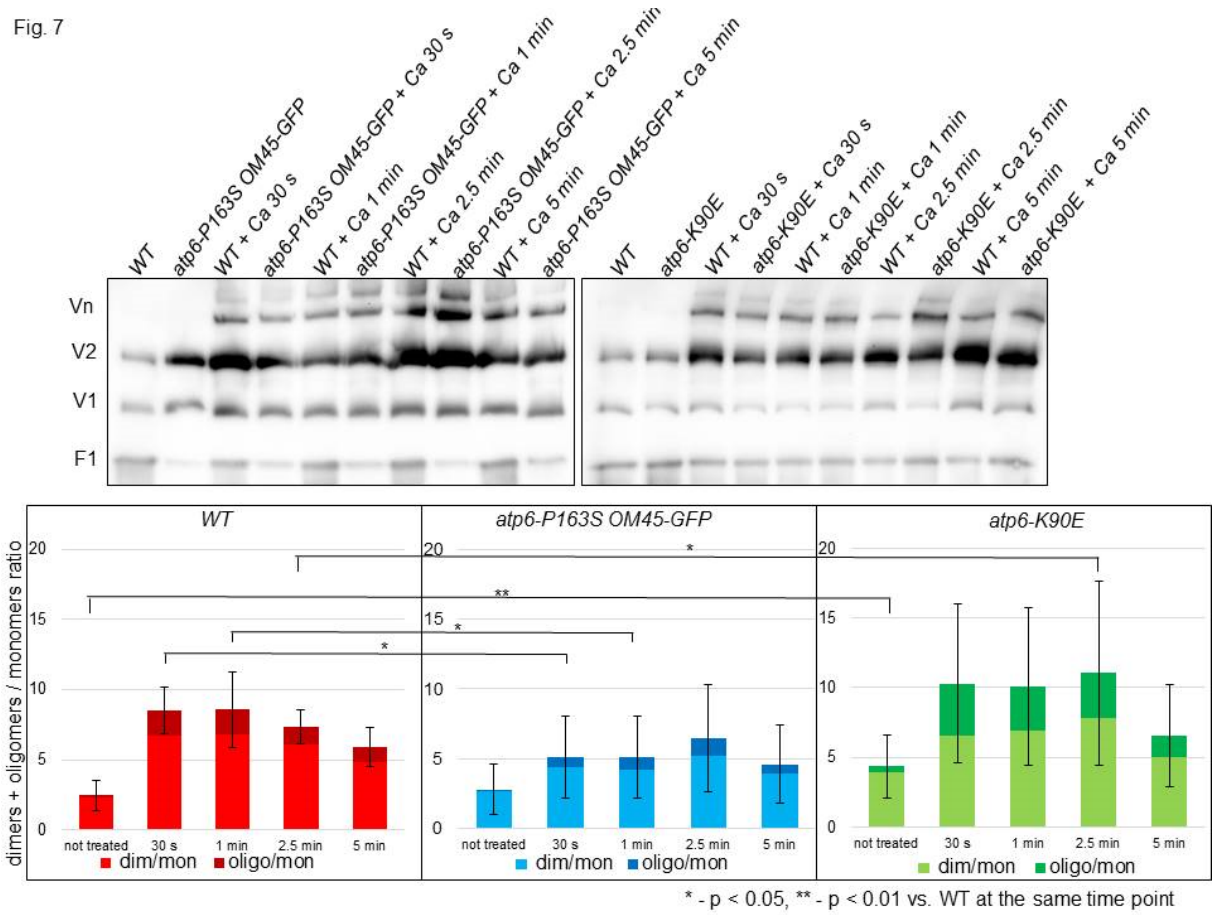


**Fig. 7. The differences in ATP synthase dimers and oligomers formation during permeability transition in yeast mitochondria.** 450 µg of protein from isolated mitochondria was suspended in 1.5 ml of PTP buffer at 28°C and 100 µM $CaCl_2$ was added. In every time-point, a 1.33 ml aliquot of the reaction was collected and subjected to the ATP synthase complexes extraction. 160 µg of protein/lane was loaded into NativePAGE™ 3-12% Bis-Tris Gel and after migration, followed by Western blotting with anti-ATP synthase Atp2 subunit antibody. The upper panels show representative gels. Oligomeric (Vn), dimeric ($V_2$) and monomeric ($V_1$) $F_1F_O$ complexes corresponding signals are indicated. The ratio of dimeric/oligomeric to the monomeric forms of the enzyme in each sample was calculated on image density results obtained using ImageJ. The standard errors and p-values were calculated from results of at least four independent experiments. The asterisks indicate the statistical significance of the difference between mutants and wild type control at the same time point.

## 4. Discussion

Mitochondrial DNA mutations have recently attracted interest because of their high frequency in tumors. It was postulated that studies should concentrate more on OXPHOS dysfunction associated with a specific mutation [107]. Our work, focused on cancer-related mutations in *ATP6* gene of ATP synthase, showed that one of five mutations modeled in yeast cells - *atp6-P163S* (equivalent to human m.8932C>T; MTATP6-P136S) reduced OXPHOS activity to 50% at elevated temperature (Fig. 3, [28]). Here we report, that two of these mutations: *atp6-K90E* and *atp6-P163S*, (corresponding to mutations m.8716A>G and m.8932C>T of human mtDNA, found in thyroid or prostate cancer) may be significant for cancer biology, although not due to OXPHOS activity impairment. In fact, both mutations affect ROS signaling, calcium homeostasis and permeability transition pore induction by calcium when functioning of porin complex in mitochondrial outer membrane is disturbed by GFP tag fused to its component Om45p [75].

The single *OM45-GFP* mutation is not neutral for mitochondrial functions. It leads to reduction of respiration and ATP synthesis and to elevated ROS level under glucose de-repression or respiration conditions. Thus, Om45p-GFP should not be considered as marker for mitochondria in mitophagy analysis, although the mutation itself does not actually change the mitophagy rate in our experimental conditions [65]. Combining the *OM45-GFP* mutation with either *atp6-P163S* or *atp6-K90E* mutation elicits much stronger effects for yeast cells than each single mutation. This includes high ROS level, also in fermentative conditions, and deregulation of calcium homeostasis leading to growth defects, already on complete media at elevated temperature. Suppression of growth defect either by overexpression of calcium pumps or by ROS scavengers and lack of growth phenotype in single *OM45-GFP* mutant, in which ROS accumulate but calcium homeostasis is normal, suggest an additive effect of high ROS and calcium homeostasis defects on double mutant cells fitness. We have no explanation why higher ROS level in single *OM45-GFP* cells does not cause calcium deregulation, but appearance of this phenotype in *atp6* mutants underline the ATP synthase role in this process.

In yeast cells calcium concentration in cytosol increases upon different stimuli such as environmental stresses, pheromones, nutrient availability, cell wall damage, [108]. In response to higher calcium concentration calcineurin is activated to reduce

the cytosolic calcium concentration to the basal level [109]. It induces the expression of a set of $Ca^{2+}$-calcineurin – dependent target genes, including those encoding Pmc1p and Pmr1p transporters, and directly inhibits the function of vacuolar $Ca^{2+}/H^{+}$ exchanger, Vcx1p [110, 111]. The *atp6-P163S OM45-GFP* double mutant is unable to keep normal low cytosolic calcium level, which should activate calcineurin, while it is the opposite: calcineurin activity is lower, but the steady-state level of calcium pumps Pmr1p, Pmc1p, Vcx1p or Yvc1p is comparable to that in wild type cells. In *atp6-K90E OM45-GFP* mutant, only mitochondrial concentration of calcium is higher, and the down-regulation of calcineurin take place only when mitochondrial functions are derepressed – i.e. in galactose medium. Thus, it seems that the same mechanism is leading to lower activity of calcineurin in both mutants, and subsequent de-regulation of calcium pumps activity rather than expression, may be the cause of higher calcium concentration. This activity may be affected by ROS level, which is higher in *atp6-P163S OM45-GFP*, correlating with more pronounced phenotypes than in *atp6-K90E OM45-GFP* mutant. Moreover, Pmr1p, Pmc1p, Yvc1p and catalytic calcineurin subunit Cna1p proteins are very rich in cysteines, suggesting their redox state may influence their activity [112]. The participation of Por1p in regulation of calcineurin activity - direct or through other proteins, like kinases - may not be excluded [113]. Calcium increase is probably originated from inside the cell, as an addition of EGTA to the calcium rich medium cannot suppress the calcium sensitivity (Fig. 4A). Our results, in accordance with the literature, indicate that an increase in cytosolic calcium concentration mediates the cytosolic effect of oxidative stress [114, 115].

Elevated ROS and calcium concentration in the mitochondrial matrix are prominent inducers of the permeability transition [44]. ATP synthase dimers are postulated to form the core of the PTP basing on the *in vitro* experiments by the group of Paolo Bernardi [56, 57, 102, 103]. The experimental verification of PTP channel formation by ATP synthase dimers in intact cells is still lacking, but our data on isolated yeast mitochondria are in agreement with this hypothesis. Since yeast does not possess any MCU (mitochondrial calcium uniporter) identified to date, that would be responsible for rapid equilibration of calcium across the inner membrane, whether increased intracellular calcium/ROS levels can be the cause of mitochondrial outer membrane permeabilization in this organism is still under debate [40]. Our data not only supports the existence of calcium/ROS induced permeability transition in yeast, but also provides the first demonstration that ATP synthase and Por1p-Om14p-Om45p

protein complexes are involved in this process in isolated mitochondria. The regulatory role of yeast Por1p during yPTP induction had already been shown and it was postulated that the external calcium binding site is located within Por1p and that calcium binding to this site promotes closure of the channel [116]. Our data are in accordance with this paper as we observe a delay in yPTP induction when porin complex is somehow defective due to Om45p protein modification by GFP. Moreover we have shown that yPTP induction by calcium is dependent on ATP synthase alone, and more effective in *atp6-K90E* mutant mitochondria. It is possible that the structural remodeling of ATP synthase during permeability transition results in complexes different from those which are part of respirasomes during ATP production [117]. Further studies, with the use of more sophisticated methods, are necessary to verify this hypothesis.

The lower hydrolytic activity of ATP synthase mutants in *OM45-GFP* background, which is used when the mitochondrial inner membrane potential drops [118, 119] – may be also a consequence of deregulation of ROS/calcium signaling. The ATPase activity of ATP synthase is inhibited by the inhibitor protein Inh1 (IF1) whose binding to catalytic sector of ATP synthase in a ratio 1:1 is optimal under energy deficiency [120], which is not greater than the ratio observed in the single *OM45-GFP* or *atp6-P163S* mutant (Fig. 3B). IF1 protein binds to calmodulin and this binding, regulated by low micromolar $Ca^{2+}$, may regulate IF1 import into mitochondria [121]. The BN-PAGE analysis has showed that the amount of this protein bound to $F_1$ complexes is not different from the wild type enzyme, suggesting rather an IF1 heperactivation. Higher calcium concentration in the double mutants may deregulate calmodulin binding to IF1 and consequently increase its activity, but this possibility needs further experimental verification. Why two mutations (*atp6-K90E* and *atp6-P163S*) having different impact on ATP synthase activity result in the same growth phenotypes in *OM45-GFP* background [122]? *In vacuo* structural analysis has showed that both mutations may have the same effect on the structure of Atp6 subunit, mainly in the amino acid region containing the P163 (supplementary results, Fig. S5). Thus, it is possible that observed phenotypes of both *atp6-P163S* and *atp6-K90E* mutants, especially high calcium concentration in cytosol and matrix, result from distortion of this fragment of Atp6p.

The observed yPTP channel induction delay in two ATP synthase mutants, but in the *OM45-GFP* background, is very interesting, as corresponding *atp6* mutations

were found in cancer samples [76, 123] and Om45p is in a complex with the yeast VDAC homologue – Por1p [62]. In mammals, silencing VDAC inhibits PTP opening and protects cells from cell death, while its overexpression triggers PTP opening and induces apoptosis [81, 124]. VDAC proteins are overexpressed in many types of cancer cells, as well as hexokinase II (HKII), which binds to it on the mitochondrial membrane [125, 126]. Overexpression of VDAC together with HKII favors glycolysis (Warburg effect) and the protection against cells death [127, 128]. Thus, the role of VDAC as a modulator of PTP in cancer progression is supported by many experimental proofs, while the significance of mtDNA mutations for cancer remains still unclear. Many researchers consider that mtDNA mutations are rather a consequence of deregulation of ROS homeostasis in cancers and its mutagenic activity [129]. Others consider that mitochondrial dysfunctions, caused by mtDNA mutations, may initiate a complex cellular reprogramming that supports the formation and progression of cancers [14]. Here, we present evidence that mtDNA mutations selected during carcinogenesis may play a role in cancer specific cellular reprogramming. We propose the following scenario in the double mutants. Por1p complex function is inhibited by GFP, transport of metabolites into the mitochondria is less effective, which impinges on OXPHOS efficiency and raises ROS level, especially under respiratory conditions (Fig. 8). Interference on ATP synthase structural dynamics by the mutations in Atp6p, could activate a mitochondrial signaling cascade, through calcium accumulation in the mitochondrial matrix and the deregulation of the ROS/calcium/calcineurin signaling in the cell. Por1p complex tampering and ATP synthase dysfunction/structural changes caused by mutations have additive effect on desensitization of PTP to calcium while the single mutations have no effect (*OM45-GFP, atp6-P163S*) or the opposite one (*atp6-K90E*). Thus in cancer cell genetic background, often characterized by the presence of many nuclear mutations, these mtDNA mutations may be beneficial for proliferation and thus would be preserved.

The results of our research are relevant from a medical point of view. Research to develop anti-cancer drugs that silence the expression of VDAC is already under way and is promising. Silencing VDAC by shRNA or VDAC-based peptides resulted in the induction of apoptosis in tumor cells [130-132]. Recent data focused the attention on ATP synthase as a therapeutic target, for instance observation that apoptosis inducing drug (i.e. apoptolidin) acts by inhibiting ATP synthase or that oligomycin modulates the pro-apoptotic action of TNF [133, 134]. Our results indicate that simultaneous targeting

of both VDAC and ATP synthase may be more effective in the activation of apoptosis than the modulation of activity of single complex. Nevertheless, development of such a therapeutic strategy needs further understanding of the molecular mechanisms of interaction between these two complexes, important for PTP induction.

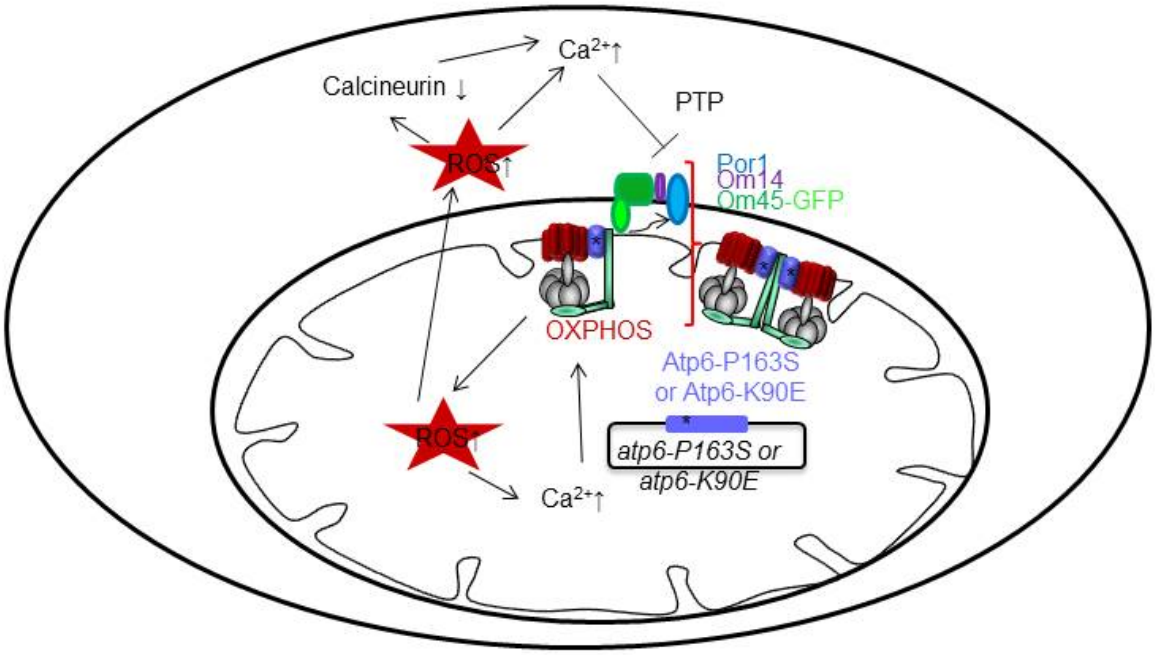


**Fig. 8. The consequences of defective interaction between ATP synthase and porin complex in yeast cell**. Defective functioning of both complexes, because of point Atp6p mutations and GFP tag at the Om45p, results in higher ROS and calcium level in the matrix and in the cytosol, likely due to higher release from an internal compartment. This is accompanied by a decrease in calcineurin activity by an unknown mechanism, which, although the amount of calcium transporters in the cell is unchanged, impairs the recovery of normal calcium concentrations. The higher calcium concentration persists in the cell and desensitizes yPTP for calcium. This inhibition may result from defective changes in ATP synthase structure during yPTP induction by matrix calcium and simultaneous inhibition of yPTP by porin, which has been proposed to bind cytosolic calcium in this process.

**Acknowledgements**

The authors thank very much prof. Christos Chinopoulos for the help in the establishment of CRC and PTP assays in their laboratory and the critical reading of the manuscript; Dr Pierre Morsomme for the antibodies against Vcx1p, Yvc1p, Pmr1p

and Pmc1p; Rodney Devenish for mt-Rosella plasmid; and Dr Alain Dautant for the help in the Fig.1 preparation.

## Competing interests

The authors declare no competing or financial interests.

## Author contributions

K.N. performed all experiments, analysis of the data and contributed to the preparation of the manuscript. R.T. designed experiment of calcium concentration and calcineurin activity measurement and contributed to writing of the manuscript. S.P. performed the calcium concentration measurement. D.P. performed analysis *in vacuo* and wrote this part of the results. M.L. monitored the swelling of mitochondria under confocal microscopy. RK constructed the mitochondrial mutants, designed the experiments, analyzed the data and wrote the manuscript.

## Funding

This work was supported by the National Science Centre of Poland nr 2013/11/B/NZ1/02102 to R.K.

## References


[1] P.D. Boyer, The binding change mechanism for ATP synthase--some probabilities and possibilities, Biochimica et biophysica acta, 1140 (1993) 215-250.

[2] H. Noji, R. Yasuda, M. Yoshida, K. Kinosita, Jr., Direct observation of the rotation of F1-ATPase, Nature, 386 (1997) 299-302.

[3] J.L. Rubinstein, J.E. Walker, R. Henderson, Structure of the mitochondrial ATP synthase by electron cryomicroscopy, The EMBO journal, 22 (2003) 6182-6192.

[4] J.P. Abrahams, A.G. Leslie, R. Lutter, J.E. Walker, Structure at 2.8 A resolution of F1-ATPase from bovine heart mitochondria, Nature, 370 (1994) 621-628.

[5] V.K. Dickson, J.A. Silvester, I.M. Fearnley, A.G. Leslie, J.E. Walker, On the structure of the stator of the mitochondrial ATP synthase, The EMBO journal, 25 (2006) 2911-2918.

[6] D.M. Rees, A.G. Leslie, J.E. Walker, The structure of the membrane extrinsic region of bovine ATP synthase, Proceedings of the National Academy of Sciences of the United States of America, 106 (2009) 21597-21601.

[7] Y. Sambongi, Y. Iko, M. Tanabe, H. Omote, A. Iwamoto-Kihara, I. Ueda, T. Yanagida, Y. Wada, M. Futai, Mechanical rotation of the c subunit oligomer in ATP synthase (F0F1): direct observation, Science, 286 (1999) 1722-1724.

[8] S.P. Tsunoda, R. Aggeler, M. Yoshida, R.A. Capaldi, Rotation of the c subunit oligomer in fully functional F1Fo ATP synthase, Proceedings of the National Academy of Sciences of the United States of America, 98 (2001) 898-902.

[9] K.M. Davies, C. Anselmi, I. Wittig, J.D. Faraldo-Gomez, W. Kuhlbrandt, Structure of the yeast F1Fo-ATP synthase dimer and its role in shaping the mitochondrial cristae, Proceedings of the National Academy of Sciences of the United States of America, 109 (2012) 13602-13607.

[10] P. Paumard, J. Vaillier, B. Coulary, J. Schaeffer, V. Soubannier, D.M. Mueller, D. Brethes, J.P. di Rago, J. Velours, The ATP synthase is involved in generating mitochondrial cristae morphology, The EMBO journal, 21 (2002) 221-230.

[11] M. Strauss, G. Hofhaus, R.R. Schroder, W. Kuhlbrandt, Dimer ribbons of ATP synthase shape the inner mitochondrial membrane, The EMBO journal, 27 (2008) 1154-1160.

[12] R.W. Taylor, D.M. Turnbull, Mitochondrial DNA mutations in human disease, Nature reviews. Genetics, 6 (2005) 389-402.

[13] K. Hejzlarova, T. Mracek, M. Vrbacky, V. Kaplanova, V. Karbanova, H. Nuskova, P. Pecina, J. Houstek, Nuclear genetic defects of mitochondrial ATP synthase, Physiological research, 63 Suppl 1 (2014) S57-71.

[14] C.C. Hsu, L.M. Tseng, H.C. Lee, Role of mitochondrial dysfunction in cancer progression, Exp Biol Med (Maywood), 241 (2016) 1281-1295.

[15] J. Lu, L.K. Sharma, Y. Bai, Implications of mitochondrial DNA mutations and mitochondrial dysfunction in tumorigenesis, Cell research, 19 (2009) 802-815.

[16] E. Morava, R.J. Rodenburg, F. Hol, M. de Vries, A. Janssen, L. van den Heuvel, L. Nijtmans, J. Smeitink, Clinical and biochemical characteristics in patients with a high mutant load of the mitochondrial T8993G/C mutations, American journal of medical genetics. Part A, 140 (2006) 863-868.

[17] A. Baracca, G. Sgarbi, M. Mattiazzi, G. Casalena, E. Pagnotta, M.L. Valentino, M. Moggio, G. Lenaz, V. Carelli, G. Solaini, Biochemical phenotypes associated with the mitochondrial ATP6 gene mutations at nt8993, Biochimica et biophysica acta, 1767 (2007) 913-919.

[18] A.E. Castagna, J. Addis, R.R. McInnes, J.T. Clarke, P. Ashby, S. Blaser, B.H. Robinson, Late onset Leigh syndrome and ataxia due to a T to C mutation at bp 9,185 of mitochondrial DNA, American journal of medical genetics. Part A, 143A (2007) 808-816.

[19] R. Carrozzo, T. Rizza, A. Stringaro, R. Pierini, E. Mormone, F.M. Santorelli, W. Malorni, P. Matarrese, Maternally-inherited Leigh syndrome-related mutations bolster mitochondrial-mediated apoptosis, Journal of neurochemistry, 90 (2004) 490-501.

[20] J.P. Lasserre, A. Dautant, R.S. Aiyar, R. Kucharczyk, A. Glatigny, D. Tribouillard-Tanvier, J. Rytka, M. Blondel, N. Skoczen, P. Reynier, L. Pitayu, A. Rotig, A. Delahodde, L.M. Steinmetz, G. Dujardin, V.

924 Procaccio, J.P. di Rago, Yeast as a system for modeling mitochondrial disease mechanisms and
925 discovering therapies, Disease models & mechanisms, 8 (2015) 509-526.
926 [21] M.V. Berridge, L. Dong, J. Neuzil, Mitochondrial DNA in Tumor Initiation, Progression, and
927 Metastasis: Role of Horizontal mtDNA Transfer, Cancer research, 75 (2015) 3203-3208.
928 [22] A.M. Kabala, J.P. Lasserre, S.H. Ackerman, J.P. di Rago, R. Kucharczyk, Defining the impact on
929 yeast ATP synthase of two pathogenic human mitochondrial DNA mutations, T9185C and T9191C,
930 Biochimie, 100 (2014) 200-206.
931 [23] R. Kucharczyk, N. Ezkurdia, E. Couplan, V. Procaccio, S.H. Ackerman, M. Blondel, J.P. di Rago,
932 Consequences of the pathogenic T9176C mutation of human mitochondrial DNA on yeast
933 mitochondrial ATP synthase, Biochimica et biophysica acta, 1797 (2010) 1105-1112.
934 [24] R. Kucharczyk, M.F. Giraud, D. Brethes, M. Wysocka-Kapcinska, N. Ezkurdia, B. Salin, J. Velours,
935 N. Camougrand, F. Haraux, J.P. di Rago, Defining the pathogenesis of human mtDNA mutations using
936 a yeast model: the case of T8851C, The international journal of biochemistry & cell biology, 45 (2013)
937 130-140.
938 [25] R. Kucharczyk, M. Rak, J.P. di Rago, Biochemical consequences in yeast of the human
939 mitochondrial DNA 8993T>C mutation in the ATPase6 gene found in NARP/MILS patients, Biochimica
940 et biophysica acta, 1793 (2009) 817-824.
941 [26] R. Kucharczyk, B. Salin, J.P. di Rago, Introducing the human Leigh syndrome mutation T9176G
942 into Saccharomyces cerevisiae mitochondrial DNA leads to severe defects in the incorporation of
943 Atp6p into the ATP synthase and in the mitochondrial morphology, Human molecular genetics, 18
944 (2009) 2889-2898.
945 [27] R. Kucharczyk, M. Zick, M. Bietenhader, M. Rak, E. Couplan, M. Blondel, S.D. Caubet, J.P. di Rago,
946 Mitochondrial ATP synthase disorders: molecular mechanisms and the quest for curative therapeutic
947 approaches, Biochimica et biophysica acta, 1793 (2009) 186-199.
948 [28] K. Niedzwiecka, A.M. Kabala, J.P. Lasserre, D. Tribouillard-Tanvier, P. Golik, A. Dautant, J.P. di
949 Rago, R. Kucharczyk, Yeast models of mutations in the mitochondrial ATP6 gene found in human
950 cancer cells, Mitochondrion, 29 (2016) 7-17.
951 [29] S. Wen, K. Niedzwiecka, W. Zhao, S. Xu, S. Liang, X. Zhu, H. Xie, D. Tribouillard-Tanvier, M.F.
952 Giraud, C. Zeng, A. Dautant, R. Kucharczyk, Z. Liu, J.P. di Rago, H. Chen, Identification of G8969>A in
953 mitochondrial ATP6 gene that severely compromises ATP synthase function in a patient with IgA
954 nephropathy, Scientific reports, 6 (2016) 36313.
955 [30] T.N. Seyfried, L.M. Shelton, Cancer as a metabolic disease, Nutrition & metabolism, 7 (2010) 7.
956 [31] O. Warburg, On respiratory impairment in cancer cells, Science, 124 (1956) 269-270.
957 [32] N. Bellance, G. Benard, F. Furt, H. Begueret, K. Smolkova, E. Passerieux, J.P. Delage, J.M. Baste, P.
958 Moreau, R. Rossignol, Bioenergetics of lung tumors: alteration of mitochondrial biogenesis and
959 respiratory capacity, The international journal of biochemistry & cell biology, 41 (2009) 2566-2577.
960 [33] S. Rodriguez-Enriquez, L. Carreno-Fuentes, J.C. Gallardo-Perez, E. Saavedra, H. Quezada, A. Vega,
961 A. Marin-Hernandez, V. Olin-Sandoval, M.E. Torres-Marquez, R. Moreno-Sanchez, Oxidative
962 phosphorylation is impaired by prolonged hypoxia in breast and possibly in cervix carcinoma, The
963 international journal of biochemistry & cell biology, 42 (2010) 1744-1751.
964 [34] E. Rodrigues-Silva, E.S. Siqueira-Santos, J.S. Ruas, R.S. Ignarro, T.R. Figueira, F. Rogerio, R.F.
965 Castilho, Evaluation of mitochondrial respiratory function in highly glycolytic glioma cells reveals low
966 ADP phosphorylation in relation to oxidative capacity, Journal of neuro-oncology, 133 (2017) 519-
967 529.
968 [35] C.E. Wenner, Targeting mitochondria as a therapeutic target in cancer, Journal of cellular
969 physiology, 227 (2012) 450-456.
970 [36] F. Weinberg, R. Hamanaka, W.W. Wheaton, S. Weinberg, J. Joseph, M. Lopez, B. Kalyanaraman,
971 G.M. Mutlu, G.R. Budinger, N.S. Chandel, Mitochondrial metabolism and ROS generation are
972 essential for Kras-mediated tumorigenicity, Proceedings of the National Academy of Sciences of the
973 United States of America, 107 (2010) 8788-8793.
974 [37] A.V. Kudryavtseva, G.S. Krasnov, A.A. Dmitriev, B.Y. Alekseev, O.L. Kardymon, A.F. Sadritdinova,
975 M.S. Fedorova, A.V. Pokrovsky, N.V. Melnikova, A.D. Kaprin, A.A. Moskalev, A.V. Snezhkina,

Mitochondrial dysfunction and oxidative stress in aging and cancer, Oncotarget, 7 (2016) 44879-44905.
[38] M. Idelchik, U. Begley, T.J. Begley, J.A. Melendez, Mitochondrial ROS control of cancer, Seminars in cancer biology, (2017).
[39] Y. Zhang, S. Muend, R. Rao, Dysregulation of ion homeostasis by antifungal agents, Frontiers in microbiology, 3 (2012) 133.
[40] M. Carraro, P. Bernardi, Calcium and reactive oxygen species in regulation of the mitochondrial permeability transition and of programmed cell death in yeast, Cell calcium, 60 (2016) 102-107.
[41] P.S. Brookes, Y. Yoon, J.L. Robotham, M.W. Anders, S.S. Sheu, Calcium, ATP, and ROS: a mitochondrial love-hate triangle, American journal of physiology. Cell physiology, 287 (2004) C817-833.
[42] N.R. Brady, A. Hamacher-Brady, H.V. Westerhoff, R.A. Gottlieb, A wave of reactive oxygen species (ROS)-induced ROS release in a sea of excitable mitochondria, Antioxidants & redox signaling, 8 (2006) 1651-1665.
[43] M. Narita, S. Shimizu, T. Ito, T. Chittenden, R.J. Lutz, H. Matsuda, Y. Tsujimoto, Bax interacts with the permeability transition pore to induce permeability transition and cytochrome c release in isolated mitochondria, Proceedings of the National Academy of Sciences of the United States of America, 95 (1998) 14681-14686.
[44] N. Tajeddine, How do reactive oxygen species and calcium trigger mitochondrial membrane permeabilisation?, Biochimica et biophysica acta, 1860 (2016) 1079-1088.
[45] D. Siemen, M. Ziemer, What is the nature of the mitochondrial permeability transition pore and what is it not?, IUBMB life, 65 (2013) 255-262.
[46] L.Y. Li, X. Luo, X. Wang, Endonuclease G is an apoptotic DNase when released from mitochondria, Nature, 412 (2001) 95-99.
[47] J.E. Kokoszka, K.G. Waymire, S.E. Levy, J.E. Sligh, J. Cai, D.P. Jones, G.R. MacGregor, D.C. Wallace, The ADP/ATP translocator is not essential for the mitochondrial permeability transition pore, Nature, 427 (2004) 461-465.
[48] C.P. Baines, R.A. Kaiser, T. Sheiko, W.J. Craigen, J.D. Molkentin, Voltage-dependent anion channels are dispensable for mitochondrial-dependent cell death, Nature cell biology, 9 (2007) 550-555.
[49] M. Gutierrez-Aguilar, D.L. Douglas, A.K. Gibson, T.L. Domeier, J.D. Molkentin, C.P. Baines, Genetic manipulation of the cardiac mitochondrial phosphate carrier does not affect permeability transition, Journal of molecular and cellular cardiology, 72 (2014) 316-325.
[50] C.P. Baines, R.A. Kaiser, N.H. Purcell, N.S. Blair, H. Osinska, M.A. Hambleton, E.W. Brunskill, M.R. Sayen, R.A. Gottlieb, G.W. Dorn, J. Robbins, J.D. Molkentin, Loss of cyclophilin D reveals a critical role for mitochondrial permeability transition in cell death, Nature, 434 (2005) 658-662.
[51] E. Basso, L. Fante, J. Fowlkes, V. Petronilli, M.A. Forte, P. Bernardi, Properties of the permeability transition pore in mitochondria devoid of Cyclophilin D, The Journal of biological chemistry, 280 (2005) 18558-18561.
[52] K.N. Alavian, G. Beutner, E. Lazrove, S. Sacchetti, H.A. Park, P. Licznerski, H. Li, P. Nabili, K. Hockensmith, M. Graham, G.A. Porter, Jr., E.A. Jonas, An uncoupling channel within the c-subunit ring of the F1FO ATP synthase is the mitochondrial permeability transition pore, Proceedings of the National Academy of Sciences of the United States of America, 111 (2014) 10580-10585.
[53] M. Bonora, A. Bononi, E. De Marchi, C. Giorgi, M. Lebiedzinska, S. Marchi, S. Patergnani, A. Rimessi, J.M. Suski, A. Wojtala, M.R. Wieckowski, G. Kroemer, L. Galluzzi, P. Pinton, Role of the c

subunit of the FO ATP synthase in mitochondrial permeability transition, Cell Cycle, 12 (2013) 674-683.
[54] J. He, H.C. Ford, J. Carroll, S. Ding, I.M. Fearnley, J.E. Walker, Persistence of the mitochondrial permeability transition in the absence of subunit c of human ATP synthase, Proceedings of the National Academy of Sciences of the United States of America, 114 (2017) 3409-3414.
[55] W. Zhou, F. Marinelli, C. Nief, J.D. Faraldo-Gomez, Atomistic simulations indicate the c-subunit ring of the F1Fo ATP synthase is not the mitochondrial permeability transition pore, eLife, 6 (2017).
[56] V. Giorgio, S. von Stockum, M. Antoniel, A. Fabbro, F. Fogolari, M. Forte, G.D. Glick, V. Petronilli, M. Zoratti, I. Szabo, G. Lippe, P. Bernardi, Dimers of mitochondrial ATP synthase form the permeability transition pore, Proceedings of the National Academy of Sciences of the United States of America, 110 (2013) 5887-5892.
[57] S. von Stockum, V. Giorgio, E. Trevisan, G. Lippe, G.D. Glick, M.A. Forte, C. Da-Re, V. Checchetto, G. Mazzotta, R. Costa, I. Szabo, P. Bernardi, F-ATPase of Drosophila melanogaster forms 53-picosiemen (53-pS) channels responsible for mitochondrial Ca2+-induced Ca2+ release, The Journal of biological chemistry, 290 (2015) 4537-4544.
[58] V. Giorgio, V. Burchell, M. Schiavone, C. Bassot, G. Minervini, V. Petronilli, F. Argenton, M. Forte, S. Tosatto, G. Lippe, P. Bernardi, Ca2+ binding to F-ATP synthase beta subunit triggers the mitochondrial permeability transition, EMBO reports, 18 (2017) 1065-1076.
[59] M. Bonora, C. Morganti, G. Morciano, G. Pedriali, M. Lebiedzinska-Arciszewska, G. Aquila, C. Giorgi, P. Rizzo, G. Campo, R. Ferrari, G. Kroemer, M.R. Wieckowski, L. Galluzzi, P. Pinton, Mitochondrial permeability transition involves dissociation of F1FO ATP synthase dimers and C-ring conformation, EMBO reports, 18 (2017) 1077-1089.
[60] R.L. Macintosh, K.M. Ryan, Autophagy in tumour cell death, Seminars in cancer biology, 23 (2013) 344-351.
[61] A. Lyakhovich, D. Graifer, B. Stefanovie, L. Krejci, Mitochondrial dysfunction in DDR-related cancer predisposition syndromes, Biochimica et biophysica acta, 1865 (2016) 184-189.
[62] S. Roy, J. Sileikyte, B. Neuenswander, M.P. Hedrick, T.D. Chung, J. Aube, F.J. Schoenen, M.A. Forte, P. Bernardi, N-Phenylbenzamides as Potent Inhibitors of the Mitochondrial Permeability Transition Pore, ChemMedChem, 11 (2016) 283-288.
[63] S. Lauffer, K. Mabert, C. Czupalla, T. Pursche, B. Hoflack, G. Rodel, U. Krause-Buchholz, Saccharomyces cerevisiae porin pore forms complexes with mitochondrial outer membrane proteins Om14p and Om45p, The Journal of biological chemistry, 287 (2012) 17447-17458.
[64] J. Conde, G.R. Fink, A mutant of Saccharomyces cerevisiae defective for nuclear fusion, Proceedings of the National Academy of Sciences of the United States of America, 73 (1976) 3651-3655.
[65] T. Kanki, D. Kang, D.J. Klionsky, Monitoring mitophagy in yeast: the Om45-GFP processing assay, Autophagy, 5 (2009) 1186-1189.
[66] R. Kucharczyk, S. Dupre, S. Avaro, R. Haguenauer-Tsapis, P.P. Slonimski, J. Rytka, The novel protein Ccz1p required for vacuolar assembly in Saccharomyces cerevisiae functions in the same transport pathway as Ypt7p, Journal of cell science, 113 Pt 23 (2000) 4301-4311.
[67] M. Rigamonti, S. Groppi, F. Belotti, R. Ambrosini, G. Filippi, E. Martegani, R. Tisi, Hypotonic stress-induced calcium signaling in Saccharomyces cerevisiae involves TRP-like transporters on the endoplasmic reticulum membrane, Cell calcium, 57 (2015) 57-68.
[68] M. Bietenhader, A. Martos, E. Tetaud, R.S. Aiyar, C.H. Sellem, R. Kucharczyk, S. Clauder-Munster, M.F. Giraud, F. Godard, B. Salin, I. Sagot, J. Gagneur, M. Dequard-Chablat, V. Contamine, S. Hermann-Le Denmat, A. Sainsard-Chanet, L.M. Steinmetz, J.P. di Rago, Experimental relocation of the

mitochondrial ATP9 gene to the nucleus reveals forces underlying mitochondrial genome evolution, PLoS genetics, 8 (2012) e1002876.
[69] S. Groppi, F. Belotti, R.L. Brandao, E. Martegani, R. Tisi, Glucose-induced calcium influx in budding yeast involves a novel calcium transport system and can activate calcineurin, Cell calcium, 49 (2011) 376-386.
[70] D. Mijaljica, M. Prescott, R.J. Devenish, A fluorescence microscopy assay for monitoring mitophagy in the yeast Saccharomyces cerevisiae, Journal of visualized experiments : JoVE, (2011).
[71] M. Brini, R. Marsault, C. Bastianutto, J. Alvarez, T. Pozzan, R. Rizzuto, Transfected aequorin in the measurement of cytosolic Ca2+ concentration ([Ca2+]c). A critical evaluation, The Journal of biological chemistry, 270 (1995) 9896-9903.
[72] A. Gomes, E. Fernandes, J.L. Lima, Fluorescence probes used for detection of reactive oxygen species, Journal of biochemical and biophysical methods, 65 (2005) 45-80.
[73] B. Guerin, P. Labbe, M. Somlo, Preparation of yeast mitochondria (Saccharomyces cerevisiae) with good P/O and respiratory control ratios, Methods in enzymology, 55 (1979) 149-159.
[74] A.S. Colinet, P. Sengottaiyan, A. Deschamps, M.L. Colsoul, L. Thines, D. Demaegd, M.C. Duchene, F. Foulquier, P. Hols, P. Morsomme, Yeast Gdt1 is a Golgi-localized calcium transporter required for stress-induced calcium signaling and protein glycosylation, Scientific reports, 6 (2016) 24282.
[75] I. Bohovych, O. Khalimonchuk, Sending Out an SOS: Mitochondria as a Signaling Hub, Frontiers in cell and developmental biology, 4 (2016) 109.
[76] V. Maximo, P. Soares, J. Lima, J. Cameselle-Teijeiro, M. Sobrinho-Simoes, Mitochondrial DNA somatic mutations (point mutations and large deletions) and mitochondrial DNA variants in human thyroid pathology: a study with emphasis on Hurthle cell tumors, The American journal of pathology, 160 (2002) 1857-1865.
[77] S. Lorin, A. Hamai, M. Mehrpour, P. Codogno, Autophagy regulation and its role in cancer, Seminars in cancer biology, 23 (2013) 361-379.
[78] K.J. Rieger, A. Kaniak, J.Y. Coppee, G. Aljinovic, A. Baudin-Baillieu, G. Orlowska, R. Gromadka, O. Groudinsky, J.P. Di Rago, P.P. Slonimski, Large-scale phenotypic analysis--the pilot project on yeast chromosome III, Yeast, 13 (1997) 1547-1562.
[79] S. Luikenhuis, G. Perrone, I.W. Dawes, C.M. Grant, The yeast Saccharomyces cerevisiae contains two glutaredoxin genes that are required for protection against reactive oxygen species, Molecular biology of the cell, 9 (1998) 1081-1091.
[80] N.M. Mazure, VDAC in cancer, Biochimica et biophysica acta, (2017).
[81] F. Tomasello, A. Messina, L. Lartigue, L. Schembri, C. Medina, S. Reina, D. Thoraval, M. Crouzet, F. Ichas, V. De Pinto, F. De Giorgi, Outer membrane VDAC1 controls permeability transition of the inner mitochondrial membrane in cellulo during stress-induced apoptosis, Cell research, 19 (2009) 1363-1376.
[82] J.R. Rohde, R. Bastidas, R. Puria, M.E. Cardenas, Nutritional control via Tor signaling in Saccharomyces cerevisiae, Current opinion in microbiology, 11 (2008) 153-160.
[83] Y. Pan, E.A. Schroeder, A. Ocampo, A. Barrientos, G.S. Shadel, Regulation of yeast chronological life span by TORC1 via adaptive mitochondrial ROS signaling, Cell metabolism, 13 (2011) 668-678.
[84] R. Ameziane-El-Hassani, M. Boufraqech, O. Lagente-Chevallier, U. Weyemi, M. Talbot, D. Metivier, F. Courtin, J.M. Bidart, M. El Mzibri, M. Schlumberger, C. Dupuy, Role of H2O2 in RET/PTC1

chromosomal rearrangement produced by ionizing radiation in human thyroid cells, Cancer research, 70 (2010) 4123-4132.
[85] R. Mahfouz, R. Sharma, J. Lackner, N. Aziz, A. Agarwal, Evaluation of chemiluminescence and flow cytometry as tools in assessing production of hydrogen peroxide and superoxide anion in human spermatozoa, Fertility and sterility, 92 (2009) 819-827.
[86] S. Rexroth, A. Poetsch, M. Rogner, A. Hamann, A. Werner, H.D. Osiewacz, E.R. Schafer, H. Seelert, N.A. Dencher, Reactive oxygen species target specific tryptophan site in the mitochondrial ATP synthase, Biochimica et biophysica acta, 1817 (2012) 381-387.
[87] C.M. Grant, F.H. MacIver, I.W. Dawes, Mitochondrial function is required for resistance to oxidative stress in the yeast Saccharomyces cerevisiae, FEBS letters, 410 (1997) 219-222.
[88] M.D. Pereira, R.S. Herdeiro, P.N. Fernandes, E.C. Eleutherio, A.D. Panek, Targets of oxidative stress in yeast sod mutants, Biochimica et biophysica acta, 1620 (2003) 245-251.
[89] C. Busso, E.B. Tahara, R. Ogusucu, O. Augusto, J.R. Ferreira-Junior, A. Tzagoloff, A.J. Kowaltowski, M.H. Barros, Saccharomyces cerevisiae coq10 null mutants are responsive to antimycin A, The FEBS journal, 277 (2010) 4530-4538.
[90] W. Hansberg, R. Salas-Lizana, L. Dominguez, Fungal catalases: function, phylogenetic origin and structure, Archives of biochemistry and biophysics, 525 (2012) 170-180.
[91] A. Mukhopadhyay, M. Uh, D.M. Mueller, Level of ATP synthase activity required for yeast Saccharomyces cerevisiae to grow on glycerol media, FEBS letters, 343 (1994) 160-164.
[92] R. Venard, D. Brethes, M.F. Giraud, J. Vaillier, J. Velours, F. Haraux, Investigation of the role and mechanism of IF1 and STF1 proteins, twin inhibitory peptides which interact with the yeast mitochondrial ATP synthase, Biochemistry, 42 (2003) 7626-7636.
[93] S.H. Ackerman, A. Tzagoloff, Function, structure, and biogenesis of mitochondrial ATP synthase, Progress in nucleic acid research and molecular biology, 80 (2005) 95-133.
[94] J. Jacobson, M.R. Duchen, Interplay between mitochondria and cellular calcium signalling, Molecular and cellular biochemistry, 256-257 (2004) 209-218.
[95] T.I. Peng, M.J. Jou, Oxidative stress caused by mitochondrial calcium overload, Annals of the New York Academy of Sciences, 1201 (2010) 183-188.
[96] V. Adam-Vizi, A.A. Starkov, Calcium and mitochondrial reactive oxygen species generation: how to read the facts, Journal of Alzheimer's disease : JAD, 20 Suppl 2 (2010) S413-426.
[97] R. Uzhachenko, A. Shanker, W.G. Yarbrough, A.V. Ivanova, Mitochondria, calcium, and tumor suppressor Fus1: At the crossroad of cancer, inflammation, and autoimmunity, Oncotarget, 6 (2015) 20754-20772.
[98] M.S. Cyert, Calcineurin signaling in Saccharomyces cerevisiae: how yeast go crazy in response to stress, Biochemical and biophysical research communications, 311 (2003) 1143-1150.
[99] S.J. Yu, Y.L. Chang, Y.L. Chen, Calcineurin signaling: lessons from Candida species, FEMS yeast research, 15 (2015) fov016.
[100] K.A. Kafadar, M.S. Cyert, Integration of stress responses: modulation of calcineurin signaling in Saccharomyces cerevisiae by protein kinase A, Eukaryotic cell, 3 (2004) 1147-1153.
[101] P. Bernardi, F. Di Lisa, F. Fogolari, G. Lippe, From ATP to PTP and Back: A Dual Function for the Mitochondrial ATP Synthase, Circulation research, 116 (2015) 1850-1862.
[102] P. Bernardi, A. Rasola, M. Forte, G. Lippe, The Mitochondrial Permeability Transition Pore: Channel Formation by F-ATP Synthase, Integration in Signal Transduction, and Role in Pathophysiology, Physiological reviews, 95 (2015) 1111-1155.
[103] M. Carraro, V. Giorgio, J. Sileikyte, G. Sartori, M. Forte, G. Lippe, M. Zoratti, I. Szabo, P. Bernardi, Channel formation by yeast F-ATP synthase and the role of dimerization in the mitochondrial permeability transition, The Journal of biological chemistry, 289 (2014) 15980-15985.
[104] A. Yamada, T. Yamamoto, Y. Yoshimura, S. Gouda, S. Kawashima, N. Yamazaki, K. Yamashita, M. Kataoka, T. Nagata, H. Terada, D.R. Pfeiffer, Y. Shinohara, Ca2+-induced permeability transition can

be observed even in yeast mitochondria under optimized experimental conditions, Biochimica et biophysica acta, 1787 (2009) 1486-1491.
[105] E. Fontaine, F. Ichas, P. Bernardi, A ubiquinone-binding site regulates the mitochondrial permeability transition pore, The Journal of biological chemistry, 273 (1998) 25734-25740.
[106] T. Kristian, T.M. Weatherby, T.E. Bates, G. Fiskum, Heterogeneity of the calcium-induced permeability transition in isolated non-synaptic brain mitochondria, Journal of neurochemistry, 83 (2002) 1297-1308.
[107] A. Cruz-Bermudez, R.J. Vicente-Blanco, E. Gonzalez-Vioque, M. Provencio, M.A. Fernandez-Moreno, R. Garesse, Spotlight on the relevance of mtDNA in cancer, Clinical & translational oncology : official publication of the Federation of Spanish Oncology Societies and of the National Cancer Institute of Mexico, 19 (2017) 409-418.
[108] R. Tisi, M. Rigamonti, S. Groppi, F. Belotti, Calcium homeostasis and signaling in fungi and their relevance for pathogenicity of yeasts and filamentous fungi, Aims Mol Sci, 3 (2016) 505-549.
[109] S. Thewes, Calcineurin-Crz1 signaling in lower eukaryotes, Eukaryotic cell, 13 (2014) 694-705.
[110] D.P. Matheos, T.J. Kingsbury, U.S. Ahsan, K.W. Cunningham, Tcn1p/Crz1p, a calcineurin-dependent transcription factor that differentially regulates gene expression in Saccharomyces cerevisiae, Genes & development, 11 (1997) 3445-3458.
[111] K.W. Cunningham, G.R. Fink, Calcineurin inhibits VCX1-dependent H+/Ca2+ exchange and induces Ca2+ ATPases in Saccharomyces cerevisiae, Molecular and cellular biology, 16 (1996) 2226-2237.
[112] A.V. Zima, L.A. Blatter, Redox regulation of cardiac calcium channels and transporters, Cardiovascular research, 71 (2006) 310-321.
[113] V. Strogolova, M. Orlova, A. Shevade, S. Kuchin, Mitochondrial porin Por1 and its homolog Por2 contribute to the positive control of Snf1 protein kinase in Saccharomyces cerevisiae, Eukaryotic cell, 11 (2012) 1568-1572.
[114] C.V. Popa, I. Dumitru, L.L. Ruta, A.F. Danet, I.C. Farcasanu, Exogenous oxidative stress induces Ca2+ release in the yeast Saccharomyces cerevisiae, The FEBS journal, 277 (2010) 4027-4038.
[115] A. Vlahakis, N. Lopez Muniozguren, T. Powers, Calcium channel regulator Mid1 links TORC2-mediated changes in mitochondrial respiration to autophagy, The Journal of cell biology, 215 (2016) 779-788.
[116] J. Sileikyte, S. Roy, P. Porubsky, B. Neuenswander, J. Wang, M. Hedrick, A.B. Pinkerton, S. Salaniwal, P. Kung, A. Mangravita-Novo, L.H. Smith, D.N. Bourdette, M.R. Jackson, J. Aube, T.D.Y. Chung, F.J. Schoenen, M.A. Forte, P. Bernardi, Small Molecules Targeting the Mitochondrial

Permeability Transition, Probe Reports from the NIH Molecular Libraries Program, Place Published, 2010.
[117] J.A. Letts, K. Fiedorczuk, L.A. Sazanov, The architecture of respiratory supercomplexes, Nature, 537 (2016) 644-648.
[118] J. Weber, A.E. Senior, Catalytic mechanism of F1-ATPase, Biochimica et biophysica acta, 1319 (1997) 19-58.
[119] N. Ichikawa, Y. Yoshida, T. Hashimoto, N. Ogasawara, H. Yoshikawa, F. Imamoto, K. Tagawa, Activation of ATP hydrolysis by an uncoupler in mutant mitochondria lacking an intrinsic ATPase inhibitor in yeast, The Journal of biological chemistry, 265 (1990) 6274-6278.
[120] D.W. Green, G.J. Grover, The IF(1) inhibitor protein of the mitochondrial F(1)F(0)-ATPase, Biochimica et biophysica acta, 1458 (2000) 343-355.
[121] S. Contessi, F. Haraux, I. Mavelli, G. Lippe, Identification of a conserved calmodulin-binding motif in the sequence of F0F1 ATPsynthase inhibitor protein, Journal of bioenergetics and biomembranes, 37 (2005) 317-326.
[122] V. Pagadala, L. Vistain, J. Symersky, D.M. Mueller, Characterization of the mitochondrial ATP synthase from yeast Saccharomyces cerevisae, Journal of bioenergetics and biomembranes, 43 (2011) 333-347.
[123] F. Di Lisa, P. Bernardi, Modulation of Mitochondrial Permeability Transition in Ischemia-Reperfusion Injury of the Heart. Advantages and Limitations, Current medicinal chemistry, 22 (2015) 2480-2487.
[124] V. De Pinto, F. Tomasello, A. Messina, F. Guarino, R. Benz, D. La Mendola, A. Magri, D. Milardi, G. Pappalardo, Determination of the conformation of the human VDAC1 N-terminal peptide, a protein moiety essential for the functional properties of the pore, Chembiochem : a European journal of chemical biology, 8 (2007) 744-756.
[125] J.G. Pastorino, N. Shulga, J.B. Hoek, Mitochondrial binding of hexokinase II inhibits Bax-induced cytochrome c release and apoptosis, The Journal of biological chemistry, 277 (2002) 7610-7618.
[126] S. Abu-Hamad, H. Zaid, A. Israelson, E. Nahon, V. Shoshan-Barmatz, Hexokinase-I protection against apoptotic cell death is mediated via interaction with the voltage-dependent anion channel-1: mapping the site of binding, The Journal of biological chemistry, 283 (2008) 13482-13490.
[127] T. Arif, Y. Krelin, V. Shoshan-Barmatz, Reducing VDAC1 expression induces a non-apoptotic role for pro-apoptotic proteins in cancer cell differentiation, Biochimica et biophysica acta, 1857 (2016) 1228-1242.
[128] V. Shoshan-Barmatz, D. Ben-Hail, L. Admoni, Y. Krelin, S.S. Tripathi, The mitochondrial voltage-dependent anion channel 1 in tumor cells, Biochimica et biophysica acta, 1848 (2015) 2547-2575.
[129] P. Bernardi, F. Di Lisa, The mitochondrial permeability transition pore: molecular nature and role as a target in cardioprotection, Journal of molecular and cellular cardiology, 78 (2015) 100-106.
[130] D. De Stefani, A. Bononi, A. Romagnoli, A. Messina, V. De Pinto, P. Pinton, R. Rizzuto, VDAC1 selectively transfers apoptotic Ca2+ signals to mitochondria, Cell death and differentiation, 19 (2012) 267-273.
[131] L. Arzoine, N. Zilberberg, R. Ben-Romano, V. Shoshan-Barmatz, Voltage-dependent anion channel 1-based peptides interact with hexokinase to prevent its anti-apoptotic activity, The Journal of biological chemistry, 284 (2009) 3946-3955.
[132] N. Arbel, V. Shoshan-Barmatz, Voltage-dependent anion channel 1-based peptides interact with Bcl-2 to prevent antiapoptotic activity, The Journal of biological chemistry, 285 (2010) 6053-6062.
[133] A.R. Salomon, D.W. Voehringer, L.A. Herzenberg, C. Khosla, Apoptolidin, a selective cytotoxic agent, is an inhibitor of F0F1-ATPase, Chemistry & biology, 8 (2001) 71-80.
[134] L.A. Shchepina, O.Y. Pletjushkina, A.V. Avetisyan, L.E. Bakeeva, E.K. Fetisova, D.S. Izyumov, V.B. Saprunova, M.Y. Vyssokikh, B.V. Chernyak, V.P. Skulachev, Oligomycin, inhibitor of the F0 part of H+-ATP-synthase, suppresses the TNF-induced apoptosis, Oncogene, 21 (2002) 8149-8157.